Mechanics of Advanced Composite Structures 10 (2023) 343 – 362

Semnan University

Mechanics of Advanced Composite Structures

journal homepage: http://MACS.journals.semnan.ac.ir

Quick Review and Assessment of Thermal Stress Analyses for Exact and Assumed Temperature Distribution for Composite and Sandwich Laminates

S. Pendhari *, S. Harwande, S. Kulkarni, T. Vora, J. Visariya

Structural Engineering Department, Veermata Jijabai Technological Institute, Matunga, Mumbai 400 019, India.

KEYWORDS

Composites;
Laminate;
BVP;
PDE;
ODE.

ABSTRACT

A simple semi-analytical approach is used in the present studies to achieve a thermal response of composite and sandwich layered materials in stresses and displacements. Three-dimensional (3D) heat conduction formulation has been formulated as a boundary value problem (BVP) to obtain accurate through-thickness temperature variation, which is further used for thermal stress analysis. Four layered domains of composite and/or sandwich laminate with variable degrees of orthotropic and several transverse and in-plane aspect ratios have been used for numerical investigation. Exact solutions from past studies have been used for comparison with the outcomes received in the present study and proved the accuracy and efficiency of current developments. Additionally, simple constant and linear through-thickness temperature variation has been considered for stress analysis to highlight the importance and need for exact temperature distribution for thermal stress analysis of composite and sandwich laminates. The presented semi-analytical approach achieves the benefit of exact analysis and numerical analysis and leads to accuracy and computational efficiency.

1. Introduction

Advancements in technology demanded qualitative materials rather than quantities. Quality and accuracy in composites increase their uses in most of the industry. These composites comprise more than single pure substances that are macroscopically combined. Most of these engineered materials show superior performance to conventional materials like metals. Nowadays, a composite material formed by two or more materials in a macroscopic form is commonly used. These are engineered materials with specific properties that prove better than conventional materials like metals.

During manufacturing processes and service life, these laminates formed with different materials are subject to thermal stresses at the adjacent layer due to their different thermal properties. External imposed mechanical and thermal loads cause interlaminar transverse stresses, delamination in laminae layers, and fractures in the matrix in the longitudinal direction. Therefore, a precise evaluation of transverse stresses and deformation leads to milestone achievement in this area.

Pell [1] first discovered the thermal deformation of anisotropic thin plates subjected to random loading. Classical plate theory (CLT) has been used by Timoshenko and Woinowsky-Krieger [2], Boley and Weiner [3], Johns [4], Parkus [5], Burgreen [6] and Vinson [7] for the calculation of thermal stresses in beams, plates, and shell structures. Flexural response for various temperatures has been noted by Srinivas and Rao [8]. Boleys [9] has revealed the shortcoming in accessing thermal stresses in beams. Bapu Rao [10,11] developed a three-dimensional (3D) formulation for a thick isotropic plate under thermal loading. Further, Tungikar and Rao [12] extended this study and developed an exact 3D solution for orthotropic laminate. Thermal stresses of symmetric and unsymmetric laminates

* Corresponding author. Tel.: 022 24198247.
E-mail address: sspendhari@st.vjti.ac.in

DOI: 10.22075/macs.2023.24592.1359
Received 2021-09-20; Received in revised form 2023-03-09; Accepted 2023-05-01

in plane strain conditions have been highlighted by working on it by Wu and Tauchert [13]. Finite element formulation depends on the displacement model for laminate under thermal loading was developed by Reddy and Chao [14] and Reddy et al. [15]. Carrera [16] developed equivalent-single-layer (ESL) and layer-wise (LW) modeling for both classical and mixed approaches. Fourth-order displacement and stress field conditions are used to develop the thermomechanical governing equations. Several investigations [17, 18] have been carried out using four variable deformation theories for bending and vibration analysis of sandwich plates.

Burton and Noor [19] published a critical review of computational models for laminates under thermomechanical loading and showed the path for future studies for modeling higher-temperature laminates. The elastic analysis based on displacement-based higher-order shear deformation (HOSD) theories has been detailed with the help of formulation for composite plates by Jonalagadda et al. [20]. Composite laminates are analyzed with HOSD-based C0 iso-parametric FE formulation for the assumed thermal gradient. Four layered square laminates imposed to sudden uniform temperature change have been analyzed by presenting the transient heat conduction equation by Savoia and Reddy [21]. Bhaskar et al. [22] assumed a linear through-thickness thermal profile and formulated a 3Dimensional elasticity solution for cylindrical and bi-directional bending of laminate. Transverse shear stresses with the help of first-order shear deformation (FOSD) based analytical model has been presented by Rolfes et al. [23]. Abualnour et al. [24] studied thermo-mechanical bending behavior using the four-variable trigonometric plate theory. Bakoura *et al.* [25] studied the mechanical behavior of composite plates using three variable refined plate theory. Carrera [26,27] examined the thermo-mechanical response of layered, anisotropic plates by applying the temperature profile in the thickness directions. The impact of temperature profiles on the accuracy of plate models is then examined for a broad range of classical and advanced multilayered plate theories. Using the CUF and Reissner mixed variational theorem, Robaldo and Carrera [28] investigate the thermoelastic analysis of multilayered anisotropic plates (RMVT). To create the finite element (FE) matrices, the RMVT is used in conjunction with assumptions for the displacement fields in the thickness direction.

Composite and sandwich beam has been analyzed with the development of HOSD Formulation by Kapuria et al. [29] and showed their accuracy compared with the zig-zag theory. Further, Kapuria and Achary [30] developed a higher-order zig-zag theory to analyze laminated plates under thermal loading. A similar approach by Tungikar and Rao [12] has been used by Robaldo *et al.* [31], who developed an FE solution of heat conduction for stress analysis of anisotropic laminates. The sandwich plate and viscoelastic core have been analyzed to obtain buckling, damping behavior, and frequency with the help of FE analysis by incorporating CLT theory as carried out by Pradeep et al. [32]. Gherlone and Sciuva [33] have presented thermo-mechanical FE solutions using the Hermitian zig-zag theory. A semi-analytical approach has been used by Kant et al. [34,35] for layered composite and sandwich laminate analysis imposed by thermal loading. The vibration response of multilayered sandwich laminate has been calculated by Pradeep and Ganesan [36]. Pagani and Carrera [37] used a unified formulation for laminated composite beams. Large deflection and post-buckling analyses of laminated composite with the help of a dual-phase-lag model of generalized thermoelasticity interaction in a three-dimensional homogeneous and isotropic sandwich structure have been investigated by Sur and Kanoria [38]. Garg and Chalak [39] review the analysis of the laminated composite and sandwich structures under hygrothermal conditions. Further, Garg and Chalak [40] analyze non-skew and skew laminated composite and sandwich plates subjected to hygro-thermo-mechanical conditions. Naik and Sayyad [41] developed a higher-order displacement model for calculating the cylindrical bending of laminated and sandwich plates subjected to Environmental loads.

Kant and Shiyekar [42] considered linear through-thickness temperature variation and obtained an HOSD-based analytical formulation by incorporating the impact of shear deformation and transverse normal thermal strain. Trigonometric shear deformation theory has been used for the flexural analysis of cross-ply laminated plates subjected to nonlinear thermal loading by Ghugal and Kulkarni [43]. Further responses obtained from CPT, FOSD, and HOSD for symmetric cross-ply laminated plates acted linear and nonlinear thermal and mechanical loads simultaneously have also been compared by Ghugal and Kulkarni [44]. Sayyad et al. [45] outlined hyperbolic shear deformation theory for thermal response in stresses and displacement. Various combination of heat conduction, convection, and radiation has been considered by Norouzi et al. [46] to develop an exact solution for a multilayer spherical fiber-reinforced composite. The optimal buckling temperature of the laminated composite skew plate has been obtained by the differential quadrature method with genetic algorithms by Parviz *et al.* [47] with FOSD formulation. Cross-ply laminated composite plate's behavior in terms of stress analysis has

been derived by Sayyad et al. [48,49] by using an exponential shear deformation theory and four variables shear deformation theory, respectively. The effect of uniform heat flux supply on the circular and non-circular plate with a circular opening in the form of stresses and displacements has been noted by Jafari and Jafari [50].

Fazzolari and Carrera [51] developed quasi-3D ESL and Zig-zag theory using Carrera's unified formulation to examine the thermal stability of FGM isotropic and sandwich plates subjected to various through-thickness temperature distributions. Various researchers [52–54] used quasi-3D HOST to analyze the bending, buckling, and vibration of FG plates resting on a viscoelastic foundation.

Researchers have put considerable effort into developing simplified and refined numerical and analytical models for thermal stress analyses of composite domains concerning the available literature. Mostly, simple linear and constant temperature gradients along the composite laminate depth were assumed and used for analyses. However, this rude assumption is not valid for composite laminates, which have been proven and reported in little research. Hence, efforts have been put into this paper to form simple and efficient semi-analytical models for governing heat conduction equations to obtain real temperature gradients along with the depth of laminated composites. The prime object of this paper is the development of a semi-analytical formulation for obtaining actual temperature variation along with stress analysis. Formulations include describing two-point BVP ruled by a group of coupled first-order ODEs (Eq. 1) within the depth of laminate.

$$\frac{d}{dX_3} X_2(X_3) = A(X_3) X_2(X_3) + p(X_3) \tag{1}$$

Further, stress analysis has been performed and reported for exact as well as for simple assumed constant and linear temperature gradients along with the laminate depth. Numerical studies have been reported and discussed for a wide range of lamination schemes and in-plane and transverse aspect ratios.

2. Mathematical Modelling

A layered laminate of depth 'd' consisting of perfectly bonded isotropic/orthotropic, linearly elastic laminae of constant depth and having length and breadth dimension (l x b) as considered in Fig. 1. All peripheral edges are simple diaphragm supported as in Table 1. The plate has been imposed by thermal load and/or mechanical load on its top surface. Any other external stresses on all surfaces are neglected here. The fibers are aligned in the lamina along the laminate reference axis 'X1' and perpendicular to it.

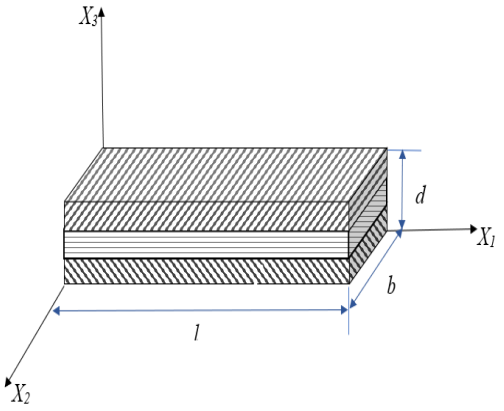

Fig. 1. 3D composite laminate

2.1. Semi-Analytical 3D Heat conduction Formulation

This section is devoted *to the* formation of a two-point boundary value problem (BVP) governed by a set of coupled ordinary differential equations (ODEs) along with the laminate thickness from the basic governing differential heat conduction Equation.

The differential heat conduction equation for a homogenous isotropic/orthotropic solid for steady-state conditions in 3D, without internal heat generation, is

$$\sum_{i=X_1,X_2,X_3} \lambda_i \frac{\partial^2 T}{\partial i^2} = 0 \tag{2}$$

Table 1. Boundary conditions (BCs)

Locations	BC imposed on the displacement field	BC imposed on the stress field
Face $X_1 = 0, l$	$v = w = 0$	_
Face $X_1 = l/2$	$u = 0$	$\tau_{X_1X_3} = 0$
Face $X_2 = 0,\ b$	$u = w = 0$	_
Face $X_2 = b/2$	$v = 0$	$\tau_{X_2X_3} = 0$.
Top face $X_3 = d/2$	-	$\tau_{X_1X_3} = \tau_{X_2X_3} = 0, \sigma_{X_3} = 0$
Bottom face $X_3 = -d/2$	-	$\tau_{X_1X_3} = \tau_{X_2X_3} = \sigma_{X_3} = 0$

According to Fourier's theory of heat conduction, heat flux in direction X_1, X_2 and X_3 is given by,

$$q_i = -\lambda_i \frac{\partial T}{\partial i} \qquad (i = X_1, X_2, X_3) \tag{3}$$

where,

λ_i = coefficient of thermal conductivity in $Wm^{-1}K^{-1}$

q_i = heat flux in Wm^{-2} and

T = temperature in Kelvin (K).

By considering total heat remains zero due to heat flow, the equilibrium equation in 3D is written as,

$$\sum_{i=X_1,X_2,X_3} \frac{\partial q_i}{\partial i} = 0 \tag{4}$$

For exact analysis in laminated layers, the continuity of heat flux and temperature at the interface must be maintained and taken care of in the present development. By using the mathematical conversion of the Equations. (2), (3), and (4), a set of partial differential equations (PDEs) includes dependent variables T and q_z, only two in quantity are derived as follows,

$$\frac{\partial}{\partial X_3}\begin{Bmatrix} T \\ q_{X_3} \end{Bmatrix} = \begin{bmatrix} 0 & -\frac{1}{\lambda_{X_3}} \\ \lambda_{X_1}\frac{\partial^2}{\partial X_1^{\,2}} + \lambda_y \frac{\partial^2}{\partial X_2^{\,2}} & 0 \end{bmatrix} \begin{Bmatrix} T \\ q_{X_3} \end{Bmatrix} \tag{5}$$

The above PDEs stated by Equation (5) can be converted to coupled first-order ODEs with the help of Fourier trigonometric series expansion for primary variables. These equations need to be

$$\begin{Bmatrix} q_{X_3}(X_1, X_2 X_3) \\ T(X_1, X_2, X_3) \end{Bmatrix} = \sum_{m,n} \begin{Bmatrix} q_{X_3}(X_3) \\ T(X_3) \end{Bmatrix} \sin\frac{m\pi X_1}{l} \sin\frac{n\pi X_2}{b} \tag{6}$$

satisfied simply supported boundary conditions at $X_1 = 0, l$ and $X_2 = 0, b$ as follows,

Substituting Equation (6) and its derivatives into Equation (5), the following set of first-order ODEs is obtained.

$$\frac{dT}{dX_3} = -\frac{q_{X_3}}{\lambda_{X_3}} \text{ and } \frac{dq_{X_3}}{dX_3} = \left(-\lambda_{X_1}\frac{m^2\pi^2}{l^2} - \lambda_{X_2}\frac{n^2\pi^2}{b^2}\right) T \tag{7}$$

Equation (7) shows the governing two-point BVP in ODEs in a domain $-d/2 \le z \le d/2$ with known temperatures at the top and bottom surfaces of a beam.

2.2. Dimensional Formulation for Stress Analysis by Semi-Analytical approach

By using the primary theory of elasticity, the material constitutive relations in 3D for each layer with reference to a laminate Cartesian coordinate system, 3D elasticity equilibrium equations, and 3D strain-displacement equations are respectively as follows,

$$\{\sigma\} = [Q]\{\varepsilon\} - [Q]\{\alpha T\} \tag{8}$$

$$\begin{aligned} &\frac{\partial \sigma_{X_1}}{\partial X_1} + \frac{\partial \tau_{X_2X_1}}{\partial X_2} + \frac{\partial \tau_{X_3X_1}}{\partial X_3} + B_{X_1} = 0 : \\ &\frac{\partial \tau_{X_1X_2}}{\partial X_1} + \frac{\partial \sigma_{X_2}}{\partial X_2} + \frac{\partial \tau_{X_3X_2}}{\partial X_3} + B_{X_2} = 0 : \\ &\frac{\partial \tau_{X_1X_3}}{\partial X_1} + \frac{\partial \tau_{X_2X_3}}{\partial X_2} + \frac{\partial \sigma_{X_3}}{\partial X_3} + B_{X_3} = 0 \end{aligned} \tag{9}$$

$$\begin{aligned} &\varepsilon_{X_1} = \frac{\partial u}{\partial X_1} \; ; \qquad \gamma_{X_1X_2} = \frac{\partial u}{\partial X_2} + \frac{\partial v}{\partial X_1} \\ &\varepsilon_{X_2} = \frac{\partial v}{\partial X_2} \; ; \qquad \gamma_{X_1X_3} = \frac{\partial u}{\partial X_3} + \frac{\partial w}{\partial X_1} \\ &\varepsilon_{X_3} = \frac{\partial w}{\partial X_3} : \qquad \gamma_{X_2X_3} = \frac{\partial v}{\partial X_3} + \frac{\partial w}{\partial X_2} \end{aligned} \tag{10}$$

in which $\{\sigma\}$ and $\{\varepsilon\}$ are the stress and strain vector correspondingly and $\{\alpha T\}$ are free thermal strains concerning laminate axes (X_1, X_2, X_3). $[Q]$ is the transformed elasticity constants matrix of the i^{th} lamina regarding the laminate axes. On performing a few algebraic operations on Equations (8)-(10) a set of partial differential equations (PDEs) that includes only eight chosen main variables $u, v, w, \tau_{X_1X_3}, \tau_{X_2X_3}$ and σ_{X_3} are obtained as,

$$\frac{\partial u}{\partial X_3} = \frac{Q_{66}}{Q_{55}Q_{66}}\tau_{X_1X_3} - \frac{\partial w}{\partial X_1}$$

$$\frac{\partial v}{\partial X_3} = \frac{\tau_{X_2X_3}}{Q_{55}Q_{66}}Q_{55} - \frac{\partial w}{\partial X_2}$$

$$\frac{\partial w}{\partial X_3} = \frac{1}{Q_{33}}\left[\sigma_{X_3} - Q_{31}\frac{\partial u}{\partial X_1} - Q_{32}\frac{\partial v}{\partial X_2}\right] + \frac{T}{Q_{33}}\begin{pmatrix} Q_{31}\alpha_{X_1} \\ +Q_{32}\alpha_y + Q_{33}\alpha_{X_3} \end{pmatrix}$$

$$\frac{\partial \tau_{X_1X_3}}{\partial X_3} = \left(-Q_{11} + \frac{Q_{13}Q_{31}}{Q_{33}}\right)\frac{\partial^2 u}{\partial X_1^{\,2}} - Q_{44}\frac{\partial^2 u}{\partial X_2^{\,2}} -$$

$$\left(Q_{12} + Q_{44} - \frac{Q_{13}Q_{32}}{Q_{33}}\right)\frac{\partial^2 v}{\partial X_1 \partial X_2} - \left(\frac{Q_{13}}{Q_{33}}\right)\frac{\partial \sigma_{X_3}}{\partial X_1} +$$

$$\begin{bmatrix} \left(Q_{11} - \frac{Q_{13}Q_{31}}{Q_{33}}\right)\alpha_{X_1} + \\ \left(Q_{12} - \frac{Q_{13}Q_{32}}{Q_{33}}\right)\alpha_{X_2} \end{bmatrix}\frac{\partial T}{\partial X_1} + \left[\alpha_{X_1X_2}Q_{44}\right]\frac{\partial T}{\partial X_2} - B_{X_1}$$

$$\frac{\partial \tau_{X_2X_3}}{\partial X_3}=\left(-Q_{22}+\frac{Q_{23}Q_{32}}{Q_{33}}\right)\frac{\partial^2 v}{\partial {X_2}^2}-$$
$$Q_{44}\frac{\partial^2 v}{\partial {X_1}^2}-\left(Q_{21}+Q_{44}-\frac{Q_{23}Q_{31}}{Q_{33}}\right)\frac{\partial^2 u}{\partial X_1\partial X_2}$$
$$-\left(\frac{Q_{23}}{Q_{33}}\right)\frac{\partial \sigma_{X_3}}{\partial X_2}+\left[\begin{matrix}\left(Q_{21}-\frac{Q_{23}Q_{31}}{Q_{33}}\right)\alpha_{X_1}+\\ \left(Q_{22}-\frac{Q_{23}Q_{32}}{Q_{33}}\right)\alpha_{X_2}\end{matrix}\right]\frac{\partial T}{\partial X_1}$$
$$+\left[Q_{44}\alpha_{X_1X_2}\right]\frac{\partial T}{\partial X_2}-B_{X_2}$$

$$\frac{\partial \sigma_{X_3}}{\partial X_3}=-\frac{\partial \tau_{X_1X_3}}{\partial X_1}-\frac{\partial \tau_{X_2X_3}}{\partial X_2}-B_{X_3} \quad (11)$$

The above PDEs stated by Equation (11) can be converted to coupled first-order ODEs by using Fourier trigonometric series expansion for primary variables satisfying the simple (diaphragm) support end conditions at X_1 = 0, l and X_2 = 0, b as shown below,

$$\left\{\begin{matrix}u(X_1,X_2,X_3)\\ \tau_{X_1X_3}(X_1,X_2,X_3)\end{matrix}\right\}=\sum_{mn}\left\{\begin{matrix}u_{mn}(X_3)\\ \tau_{X_1X_3mn}(X_3)\end{matrix}\right\}\cos\frac{m\pi X_1}{l}\sin\frac{n\pi X_2}{b}$$

$$\left\{\begin{matrix}v(X_1,X_2,X_3)\\ \tau_{X_2X_3}(X_1,X_2,X_3)\end{matrix}\right\}=\sum_{mn}\left\{\begin{matrix}v_{mn}(X_3)\\ \tau_{X_2X_3mn}(X_3)\end{matrix}\right\}\sin\frac{m\pi X_1}{l}\cos\frac{n\pi X_2}{b} \quad (12)$$

$$\left\{\begin{matrix}w(X_1,X_2,X_3)\\ \sigma_{X_3}(X_1,X_2,X_3)\end{matrix}\right\}=\sum_{mn}\left\{\begin{matrix}w_{mn}(X_3)\\ \sigma_{X_3mn}(X_3)\end{matrix}\right\}\sin\frac{m\pi X_1}{l}\sin\frac{n\pi X_2}{b}$$

where m, n=1, 3, 5, …….

Next, temperature changes along the in-plane directions are also shown in sinusoidal form as,

$$T(X_1,X_2,X_3)=\sum_{mn}^{\infty}T_{mn}(X_3)\sin\frac{m\pi X_1}{l}\sin\frac{n\pi X_2}{b} \quad (13)$$

Substituting Equations (12) and (13) and their differentiation into Equation (11), the below 6 coupled first-order Ordinary Differential Equations (ODEs) are derived.

$$\frac{du_{mn}(X_3)}{dX_3}=\left(-\frac{m\pi}{l}\right)w_{mn}(X_3)+\left(\frac{1}{Q_{55}}\right)\tau_{X_1X_3mn}(X_3)$$

$$\frac{dv_{mn}(X_3)}{dX_3}=\left(-\frac{n\pi}{b}\right)w_{mn}(X_3)+\left(\frac{1}{Q_{66}}\right)\tau_{X_2X_3mn}(X_3)$$

$$\frac{dw_{mn}(X_3)}{dX_3}=\left(\frac{m\pi}{l}\frac{Q_{31}}{Q_{33}}\right)u_{mn}(X_3)+\left(\frac{n\pi}{b}\frac{Q_{32}}{Q_{33}}\right)v_{mn}(X_3)$$
$$+\left(\frac{1}{Q_{33}}\right)\sigma_{zmn}(X_3)$$
$$+\frac{1}{Q_{33}}\left(Q_{31}\alpha_x+Q_{32}\alpha_y+Q_{33}\alpha_{X_3}\right)T(X_3)$$

$$\frac{d\tau_{X_1X_3mn}(X_3)}{dX_3}=\left[\left(Q_{11}-\frac{Q_{13}Q_{31}}{Q_{33}}\right)\frac{m^2\pi^2}{l^2}+Q_{44}\frac{n^2\pi^2}{b^2}\right]u_{mn}(X_3)$$
$$+\left(Q_{12}-\frac{Q_{13}Q_{32}}{Q_{33}}+Q_{44}\right)\frac{mn\pi^2}{lb}v_{mn}(X_3)$$
$$-\left(\frac{Q_{13}}{Q_{33}}\frac{m\pi}{a}\right)\sigma_{zmn}(X_3)-B_x(X_1,X_2,X_3)$$
$$-\left[\begin{matrix}\left(-Q_{11}+\frac{Q_{13}Q_{31}}{Q_{33}}\right)\alpha_x+\\ \left(-Q_{12}+\frac{Q_{13}Q_{32}}{Q_{33}}\right)\alpha_{X_2}\end{matrix}\right]\frac{m\pi}{l}T(X_3)$$

$$\frac{d\tau_{X_2X_3mn}(X_3)}{dX_3}=\left(Q_{21}-\frac{Q_{31}Q_{23}}{Q_{33}}+Q_{44}\right)\frac{mn\pi^2}{lb}u_{mn}(X_3)$$
$$+\left[\left(Q_{22}-\frac{Q_{23}Q_{32}}{Q_{33}}\right)\frac{n^2\pi^2}{b^2}+Q_{44}\frac{m^2\pi^2}{l^2}\right]v_{mn}(X_3)$$
$$-\left(\frac{Q_{23}}{Q_{33}}\frac{n\pi}{b}\right)\sigma_{X_3mn}(X_3)-B_y(X_1,X_2,X_3)$$
$$-\left[\begin{matrix}\left(-Q_{21}+\frac{Q_{23}Q_{31}}{Q_{33}}\right)\alpha_{X_1}+\\ \left(-Q_{22}+\frac{Q_{23}Q_{32}}{Q_{33}}\right)\alpha_y\end{matrix}\right]\frac{n\pi}{b}T(X_3)$$

$$\frac{d\sigma_{X_3mn}(X_3)}{dX_3}=\left(\frac{m\pi}{l}\right)\tau_{X_1X_3mn}(X_3)+\left(\frac{n\pi}{b}\right)\tau_{X_2X_3mn}(X_3)$$
$$-B_{X_3}(X_1,X_2,X_3) \quad (14)$$

Equation (14) represents the governing two-point BVP in ODEs in the domain $-d/2 \le X_3 \le d/2$ with stress components known at the upper and bottom surfaces of a laminate.

The solution of BVP obtained in Equations (7) and (14) are obtained by converting BVP into initial value problems (IVPs) (Tables 2 and 3). Finally, one non-homogeneous and n/2 homogeneous solution has been formed with the satisfaction of BCs at $X_3 = +d/2$, as detailed by Kant and Ramesh [55]. Changes in the material properties (Table 4) are inserted by the change in the coefficient of the material matrix appropriately during numerical integration performed by the fourth-order Runge-Kutta Gill algorithm.

Table 2. Transformation of BVP into IVPs for thermal analysis

Integration No.	Bottom edge $(X_3=-d/2)$		Top edge $(X_3=d/2)$	
	$T(X_3)$	$q_{X_3}(X_3)$	$T(X_3)$	$q_{X_3}(X_3)$
1	known	0 (assumed)	M11	M21
2	0 (assumed)	1 (assumed)	M12	M22
3 (Final)	$T(d)$ (known)	K1	$T(d)$ (known)	$q_{X_3}(d)$

Table 3. Transformation of BVP into IVPs for stress analysis

Integration No.	Starting edge; $X_3 = -d/2$						Final Edge; $X_3 = d/2$						Load term
	u	v	w	$\tau_{X_1X_3}$	$\tau_{X_2X_3}$	σ_{X_3}	u	v	w	$\tau_{X_1X_3}$	$\tau_{X_2X_3}$	σ_{X_3}	
1	0 (assumed)	0 (assumed)	0 (assumed)	0 (known)	0 (known)	0 (known)	Y_{11}	Y_{21}	Y_{31}	Y_{41}	Y_{51}	Y_{61}	Include
2	1 (unity)	0	0	0	0	0	Y_{12}	Y_{22}	Y_{32}	Y_{42}	Y_{52}	Y_{62}	Delete
3	0	1 (unity)	0	0	0	0	Y_{13}	Y_{23}	Y_{33}	Y_{43}	Y_{53}	Y_{63}	Delete
4	0	0	1 (unity)	0	0	0	Y_{14}	Y_{24}	Y_{34}	Y_{44}	Y_{54}	Y_{64}	Delete
Final	X_a	X_b	X_c	known	known	known	u_T	v_T	w_T	0	0	0	Include

Table 4. Material Properties

Set	Material Property				
I	$E_1 = E_2 =$ $E_3 = 6.9$ GPa	$\nu_{12} = \nu_{13} = \nu_{23} = 0.25$	$G_{12} = G_{13} =$ $G_{23} = 1.38$ GPa	$\alpha_1 = \alpha_2 =$ $\alpha_3 = 35.6E-6$ K^{-1}	$\lambda_1 = \lambda_2 =$ $\lambda_3 = 0.12$ W-m^{-1}K^{-1}
II	$E_1 = 224.25$ GPa $E_2 = E_3 = 6.9$ GPa	$\nu_{12} = \nu_{13} = \nu_{23} = 0.25$	$G_{12} = G_{13} = 56.58$ GPa $G_{23} = 1.38$ GPa	$\alpha_1 = 0.25E-6$ K^{-1} $\alpha_2 = \alpha_3 = 35.6E-6$ K^{-1}	$\lambda_1 = 7.2$ W-m^{-1}K^{-1} $\lambda_2 = \lambda_3 = 1.44$ W-m^{-1}K^{-1}
III	$E_1 = 172.5$ GPa $E_2 = E_3 = 6.9$ GPa	$\nu_{12} = \nu_{13} = \nu_{23} = 0.25$	$G_{12} = G_{13} = 3.45$ GPa $G_{23} = 1.38$ GPa	$\alpha_1 = 0.57E-6$ K^{-1} $\alpha_2 = \alpha_3 = 35.6E-6$ K^{-1}	$\lambda_1 = 1.92$ W-m^{-1}K^{-1} $\lambda_2 = \lambda_3 = 0.96$ W-m^{-1}K^{-1}
IV	$E_1 = 181$ GPa $E_2 = E_3 = 10.3$ GPa	$\nu_{12} = \upsilon_{13} = 0.28$ $\nu_{23} = 0.33$	$G_{12} = G_{13} = 7.17$ GPa $G_{23} = 2.87$ GPa	$\alpha_1 = 2.00E-08$ K^{-1} $\alpha_2 = \alpha_3 = 2.25E-05$ K^{-1}	$\lambda_1 = 1.5$ W-m^{-1}K^{-1} $\lambda_2 = \lambda_3 = 0.5$ W-m^{-1}K^{-1}
Face	$E_1 = 131.1$ GPa $E_2 = E_3 = 6.90$ GPa	$\nu_{12} = 0.32$ $\nu_{13} = \nu_{23} = 0.49$	$G_{12} = G_{13} = 3.588$ GPa $G_{23} = 2.332$ GPa	$\alpha_1 = 0.023E-6$ K^{-1} $\alpha_2 = \alpha_3 = 22.5E-6$ K^{-1}	$\lambda_1 = 1.5$ W-m^{-1}K^{-1} $\lambda_2 = \lambda_3 = 0.5$ W-m^{-1}K^{-1}
Core	$E_1 = 0.2208$ MPa $E_2 = 0.2001$ MPa $E_3 = 2760.0$ MPa	$\nu_{12} = 0.99$ $\nu_{13} = \upsilon_{23} = 3E-5$	$G_{12} = 16.56$ MPa $G_{13} = 545.1$ MPa $G_{23} = 455.4$ MPa	$\alpha_1 = \alpha_2 = \alpha_3 = 30.6E-6$ K^{-1}	$\lambda_1 = \lambda_2 = \lambda_3 = 3.0$ W-m^{-1}K^{-1}

λ_i = thermal conductivity coefficient $(i = 1,2,3)$

α_i = coefficient of thermal expansion $(i = 1,2,3)$

Ref: Kapuria and Acharya [30]

3. Numerical Investigation

Four, all-around simply supported composite laminates, (A), (B), (C), and (D) having different material schemes and lamination properties (Table 4) showing high in-homogeneous characteristics and variable degrees of orthotropic have been assessed for various transverse and in-plane aspect ratios. These are correlated with the real solution presented by Kapuria and Achary [30] wherever available.

A five-layered composite laminate (A) has been considered with variable in-homogenous properties for tension and shear stiffness as well as thermal coefficients and conductivity. It has individual layer thickness as $0.1d/0.25d/0.15d/0.2d/0.3d$ of material sets

I/ II/ III/ III/ III with orientations $\left[0^0/0^0/0^0/90^0/0^0\right]$.

Laminates (B) and (C) are symmetric $\left[0^0/90^0/90^0/0^0\right]$ and anti-symmetric $\left[90^0/0^0/90^0/0^0\right]$ cross-ply composites of material set IV consisting of four equal thicknesses ($0.25d$) of the lamina.

Further, five-layered sandwich laminate (D) has graphite-epoxy faces $\left[0^0/90^0\right]$ and soft-core with a thickness of each lamina as $0.05d/0.05\text{d}/0.8\text{d}/0.05d/0.05d$ has been considered.

Two different temperature cases, viz, constant temperature rise [Equation 15] along the laminate thickness simulating thermal stretching and equal rise (laminate top surface) and fall (laminate bottom surface) simulating thermal bending [Equation 16] have been considered here whereas along with in-plane directions, bidirectional sinusoidal variation is assumed [Equation 13].

$$T(X_1, X_2, \pm d/2) = T(X_3)\sin \pi X_1/l \sin \pi X_2/b \tag{15}$$

$$\begin{aligned} T(X_1, X_2, d/2) &= -T(X_1, X_2, -d/2) \\ &= T(X_3)\sin \pi X_1/l \sin \pi X_2/b \end{aligned} \tag{16}$$

For maintaining the consistency in numerical values comparison, the coefficients presented in Equation 17 have been used here for normalization.

$$\begin{aligned} &s_1 = \frac{l}{d}; \qquad \bar{\bar{u}}, \bar{v} = \frac{1}{d\,\alpha_1 T_0 s_1^3}(u; v) \\ &\bar{w} = \frac{d^3 w}{\alpha_1 T_0 l^4}; \qquad \overline{\sigma_{X_3}} = \frac{\sigma_{X_3}}{E_2 \alpha_1 T_0} \\ &\left(\overline{\sigma_{X_1}}; \overline{\sigma_{X_2}}; \overline{\tau_{X_1X_2}}\right) = \frac{1}{E_2 \alpha_1 T_0 s_1^2}\left(\sigma_{X_1}; \sigma_{X_2}; \tau_{X_1X_2}\right) \\ &\left(\overline{\tau_{X_1X_3}}; \overline{\tau_{X_2X_3}}\right) = \frac{1}{E_2 \alpha_1 T_0 s_1}\left(\tau_{X_1X_3}; \tau_{X_2X_3}\right) \end{aligned} \tag{17}$$

Firstly, heat conduction solutions have determined the exact thermal gradient for both load Case I and II, and the same has been used for thermal stress analysis (termed as Present Model 1).

Thermal stress analyses have also been performed for simple constant and linear (generally cited in literature) thermal gradient approximation (Present Model 2).

These parametric studies mainly aimed to show and compare structural responses for the exact and approximate thermal gradient. Transverse aspect ratios $\left(s_1 = l/d\right)$ ranging from thick to thin and in-plane aspect ratios $\left(s_2 = b/l\right)$ 1.5, 2, and 3 have also been considered for parametric studies, both for thermal and stress analyses.

Through thickness, thermal gradients have been presented in Figures 2 to 4 for composite laminates (A), (B), and a sandwich (D), respectively, and compared with available exact solutions (Kapuria and Achary [30]) to prove its accuracy. From Figures 2 to 4, it has been observed that thermal variation along with the depth of all composite laminates, (A), (B), and (D) remains constant for a transverse aspect ratio $\left(s_1 = l/d\right)$ of more than 20 when the domain is exposed to the thermal load case I. However, for thick and moderately thick laminates, these variations showed a considerable reduction of temperature value when compared to reference constant temperature. Nearly 60% reduction in reference temperature has been noted for all cases. In symmetric laminates, the maximum reduction is noted at the half depth of laminates (Figures 4 and 5).

In contrast, for composite laminate (A), maximum reduction (more than 70%) has been located at the height of $0.3d$ from the bottom surface. Moreover, when the domain is exposed to thermal load case II, the depth distribution of temperature depends on the lamination configuration. For symmetric composite laminate (B), thermal variation is observed to be linear, whereas, for laminates (A) and (D), a change in gradient has been observed at the lamina interfaces. However, the transverse aspect ratio effect is absent in this case.

Figures 5 to 7 depicted through depth thermal gradient for rectangular laminates. In-plane ratios affected temperature distribution along with the depth of laminates when the domain is subjected to thermal load Case I and not to thermal load Case II.

Further, obtained thermal gradient from heat conduction solutions has been used for stress analyses. Structural responses for in-plane stresses, $\left(\bar{\sigma}_{X_1}, \bar{\sigma}_{X_2}\right)$ in-plane and transverse shear stresses $\left(\bar{\tau}_{X_1X_2}, \bar{\tau}_{X_1X_3}, \bar{\tau}_{X_2X_3}\right)$, and transverse displacement $\left(\bar{w}\right)$ at silent locations for thermal stress analysis have been presented in Tables 5 to 8 for laminates A, B, C, and D, respectively.

Comparisons have been made against exact solutions presented by Kapuria and Acharya [30] and noted to match them exactly here. Moreover, an additional comparison has also been made with a Model 2 solution obtained for simple constant (Case I) and linear (Case II) thermal gradient along with the laminate depth.

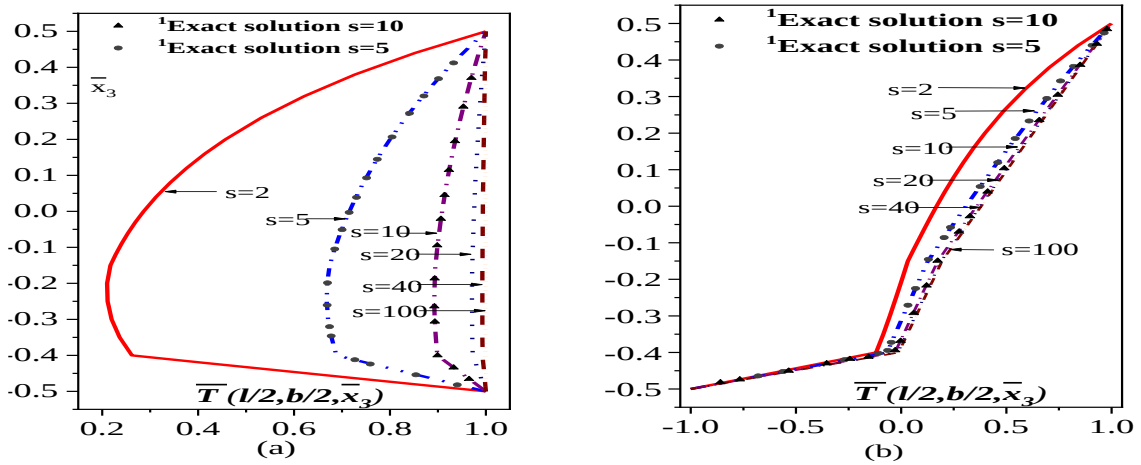

Fig. 2. Through thickness temperature variation in a five-layered symmetric composite laminate for the thermal load; (a) Case I and (b) Case II

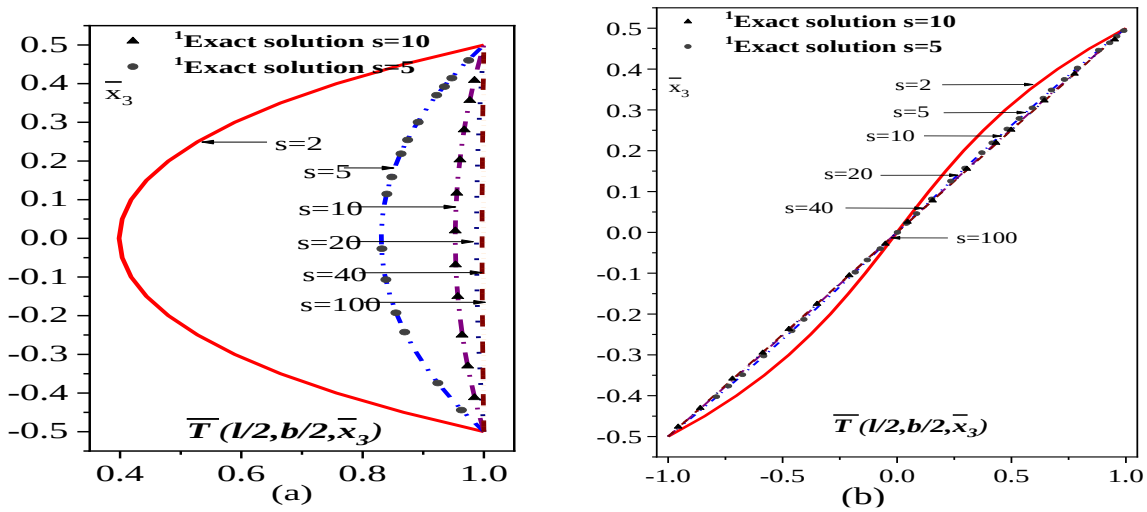

Fig. 3. Through thickness temperature variation in a four-layered symmetric composite laminate for the thermal load (a) Case I and (b) Case II

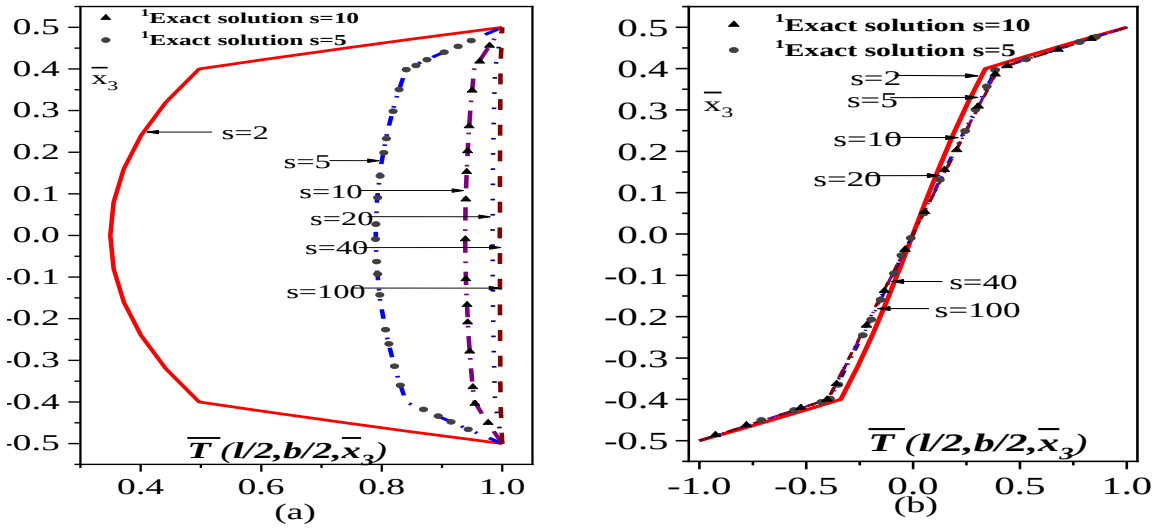

Fig. 4. Through thickness temperature variation in the five-layered sandwich composite plate for thermal load; (a) Case I and (b) Case II

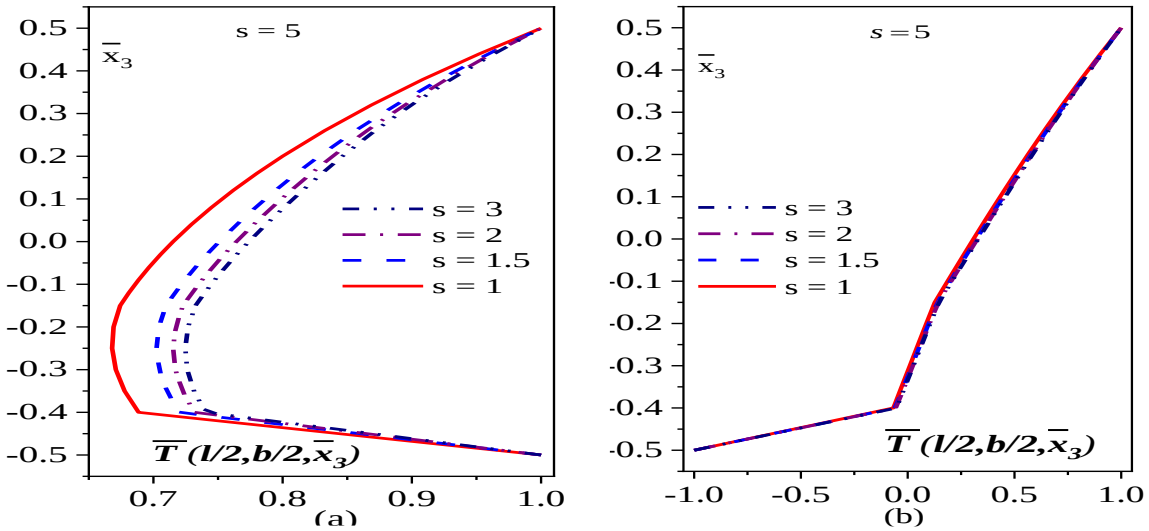

Fig. 5. Through thickness temperature variation in a five-layered rectangular symmetric $\left[0^0/0^0/0^0/90^0/0^0\right]$ composite plate for thermal load; (a) Case I and (b) Case II

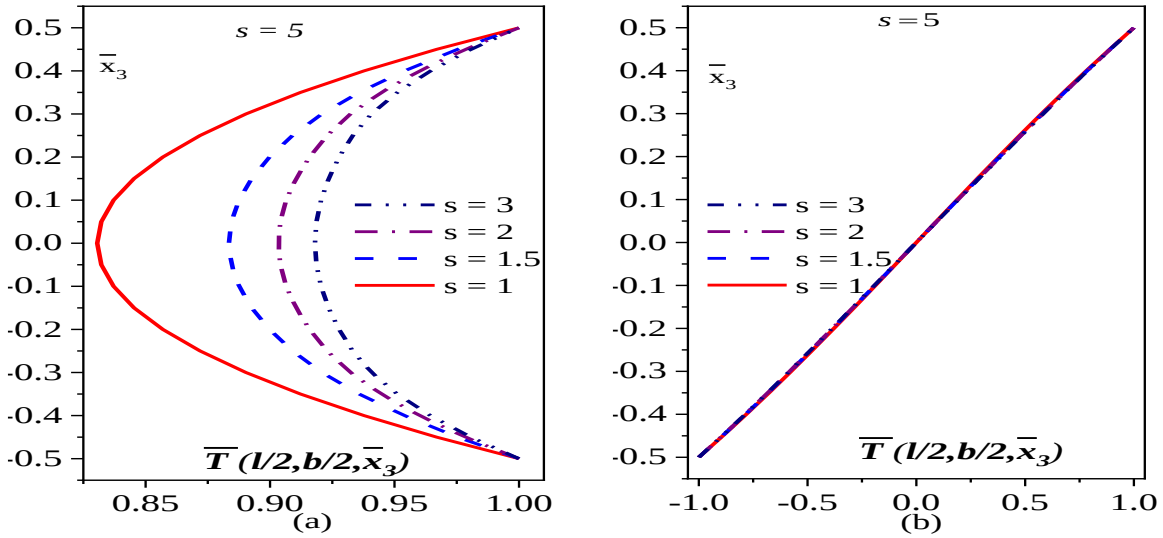

Fig. 6. Through thickness temperature variation in the four-layered rectangular symmetric composite plate for thermal load; (a) Case I and (b) Case II

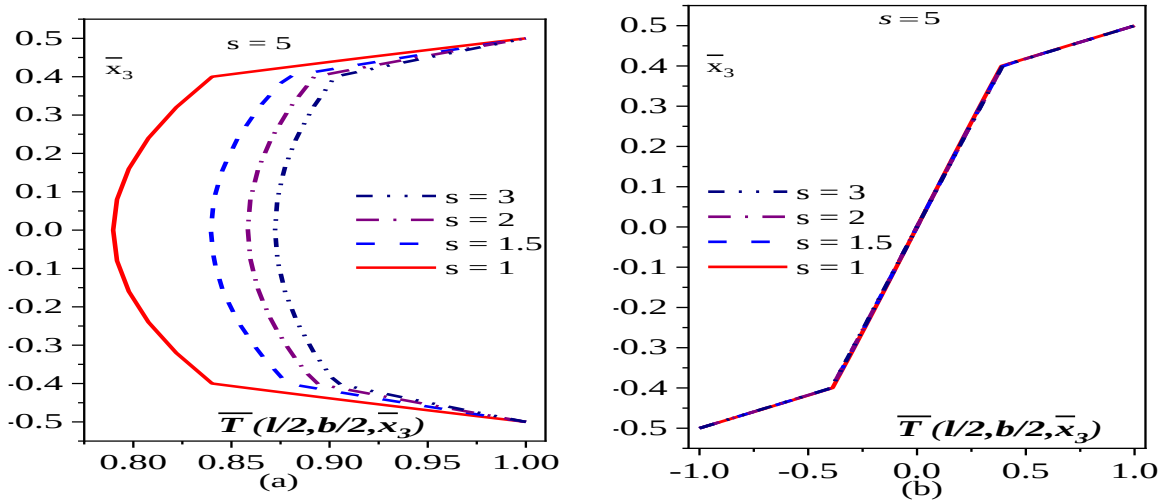

Fig. 7. Through thickness temperature variation in a five-layered rectangular sandwich composite plate for thermal load; (a) Case I and (b) Case II

For load Case I, it is worth to be noted that simple constant and linear thermal gradient assumptions and over-estimate responses for all parameters are considered here. As expected, these over-estimations are maximum for thick laminates and minimum for thin laminates. (transverse aspect ratio, s_1 > 30) as expected.

The approximate percentage differences between Model 1 and Model 2 for composite laminate (A) are 30% (in-plane stresses), 45% (transverse shear stresses), 38% (in-plane shear stress) and 45% (transverse displacement) have noted whereas, for symmetric and anti-symmetric laminates (B, C), these differences are 20% (in-plane stresses), 19% (transverse shear stresses), 12% (in-plane shear stress) and 12% (transverse displacement). For load Case II, the marginal difference between numerical values obtained from Model 1 and Model 2 analyses expects few locations to be noticed for composite laminates A, B, and C.

However, the under-estimate structural response has been observed for in-plane normal stresses and transverse shear stresses for thick laminates A. In contrast, over-estimation has been observed for transverse displacement and in-plane shear stresses.

Further, these responses have been reversed for thin composite laminates. For cross-ply symmetric and anti-symmetric composite laminates (B and C), the variation between Model 1 and Model 2 has a uniform from thick to thin laminates.

All displacements and stress parameters have been over-estimated marginally for thick laminates, whereas for thin laminates, the difference between Model 1 and Model 2 analyses has almost been nullified. Moreover, for sandwich laminate (D), the comparison between Model 1 and Model 2 numerical values showed very large differences even for thin laminates in both Cases I and II. It is established that considered temperature variation over-predicts the structural response as much as 300% for thick plates, which is minimized to approximately 135% for a thin plate with an aspect ratio greater than 30.

Through depth, variations of all displacements and stresses were available in the paper presented by Kapuria and Achary [30] and compared in present studies.

However, concerning the presented tables in the previous section, the accuracy of the current development has been very well proven. Therefore, only a few through-thickness variations showing the major discrepancy between Model 1 and Model 2 analyses have been presented in this paper for the sake of brevity. Through-thickness variations of in-plane displacement $(\bar{v})$, transverse displacement $(\bar{w})$, transverse shear stress $\left(\bar{\tau}_{X_2X_3}\right)$, and in-plane normal stress $\left(\bar{\sigma}_{X_2}\right)$ have been depicted in Figures 8 and 9 for sandwich laminate (D) subjected to Case I and II thermal loadings. Through thickness distribution of transverse stress $\left(\bar{\tau}_{X_2X_3}\right)$ and in-plane normal stress $\left(\bar{\sigma}_{X_2}\right)$ indicates a very large discrepancy and different variation patterns for the assumed thermal gradient (Model 2) when compared with Model 1. Within the core section of sandwich laminates, transverse shear stress $\left(\bar{\tau}_{X_2X_3}\right)$ shows linear and parabolic patterns for Case I and Case II when the sandwich plate is subjected to an assumed thermal gradient which is supposed to be constant as observed in Model 1 analyses. Moreover, the analysis response has shifted from positive to negative ordinates between Model 1 and Model 2.

For in-plane and transverse displacements, variation showed a similar pattern; however, major differences have been noticed between numerical values. These observations have also been noticed in other examples; however, fewer differences have been noted than sandwich laminates.

Therefore, it needs to determine the exact thermal gradient when laminates are subjected to temperature loading and mechanical loading to capture proper behavior. Simple assumptions, either constant, linear or any other patterns, will lead to wrong determination and interpretation of structural responses in laminated composites, especially composite with a high degree of orthotropic like sandwich laminates and lower transverse aspect ratios (*a/h*) that is thick laminates. Further, a selective result for rectangular plates has been presented here for future-ready reference.

Normalized in-plane normal stresses $(\bar{\sigma}_{X_1}, \bar{\sigma}_{X_2})$, transverse shear stresses $(\bar{\tau}_{X_1X_3}, \bar{\tau}_{X_2X_3})$ and the transverse displacement $(\bar{w})$ of four-layered symmetric $\left[0^0/90^0/90^0/0^0\right]$ composite rectangular (s_2 = 2) laminate have depicted in Table 9.

Through depth, changes of in-plane displacement $(\bar{v})$, transverse displacement $(\bar{w})$ transverse shear stress $\left(\bar{\tau}_{X_2X_3}\right)$, and in-plane normal stress $\left(\bar{\sigma}_y\right)$ had shown in Figures 10 and 11 for five-layered homogeneous orthotropic

laminates (A) and sandwich laminates (D) when laminates were subjected to thermal load Case I.

Additionally, changes of normalized in-plane displacement $(\bar{u})$ transverse displacement $(\bar{w})$, transverse shear stress $\left(\bar{\tau}_{X_1X_3}\right)$, and in-plane normal stress $\left(\bar{\sigma}_{X_1}\right)$ along with the thickness for four-layered symmetric (B) and anti-symmetric (C) laminates have presented in Figures 12 and 13, respectively under the applied thermal load Case II. A mixed kind of observations has been drawn from these parametric studies.

The effect of in-plane aspect ratios (b/a) has been observed for some parameters [Figure 10 (a, b, c), Figure 11 (a), Figure 12 (b, c, d), and Figure 12 (b)]. In contrast, in a few parameters, partial parts of laminate along the depth remain independent to in-plane aspect ratios, viz Figure 10 (d), Figure 11 (b, c, d), Figure 12 (a), and Figure 13 (a, c, d).

4. Conclusion

Efforts have been made to determine the exact thermal gradient for laminated plates by solving heat-conduction equations with the help of a semi-analytical approach followed by stress analyses under applied two thermal loading cases defining stretching and bending effects. The formulation depends on the formation of BVP along with the depth of laminate, and then the solution is attempted by adopting a shooting approach. Obtained thermal gradients and stress analyses result from extensive numerical studies have been compared with available solutions, and the accuracy of current development has been proved.

Further, comparisons have also been documented for simple through thickness constant and linear thermal profiles. It is observed and noted here that it is needed to capture the exact thermal profile when laminate components are subjected to thermal loading with/without other kinds of loading.

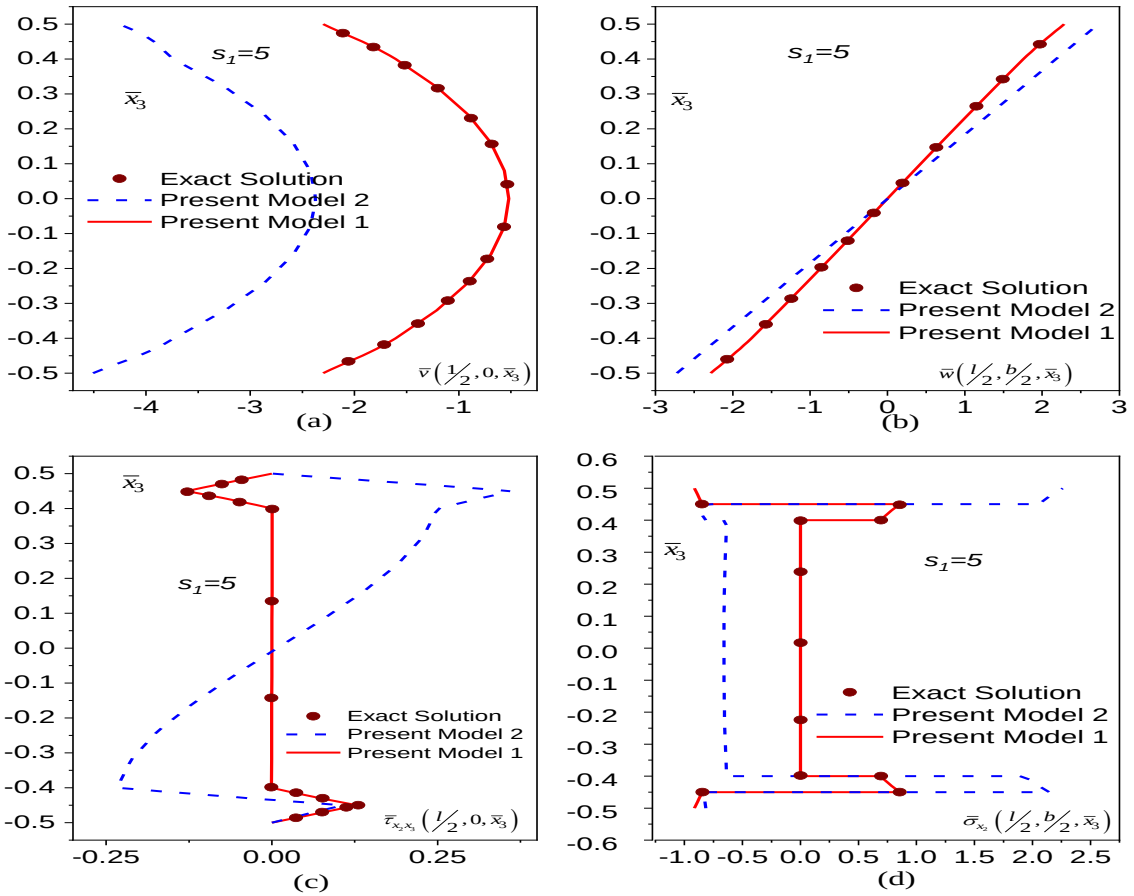

Fig. 8. Through thickness variation of normalized (a) in-plane displacement (b) transverse displacement (c) transverse shear stress (d) in-plane normal stress of five-layered sandwich composite laminate subjected to the thermal load, (Case I)

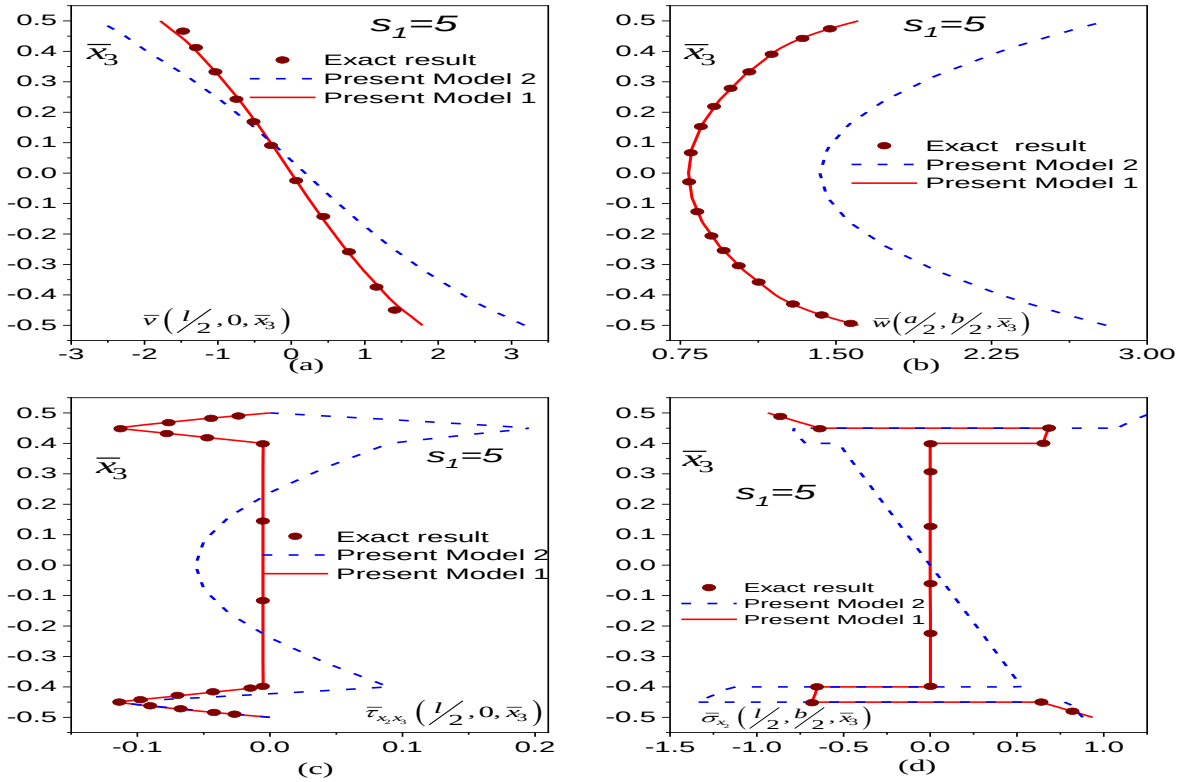

Fig. 9. Through thickness variation of normalized (a) in-plane displacement (b) transverse displacement (c) transverse shear stress (d) in-plane normal stress of five-layered sandwich composite laminate subjected to the thermal load, (Case II)

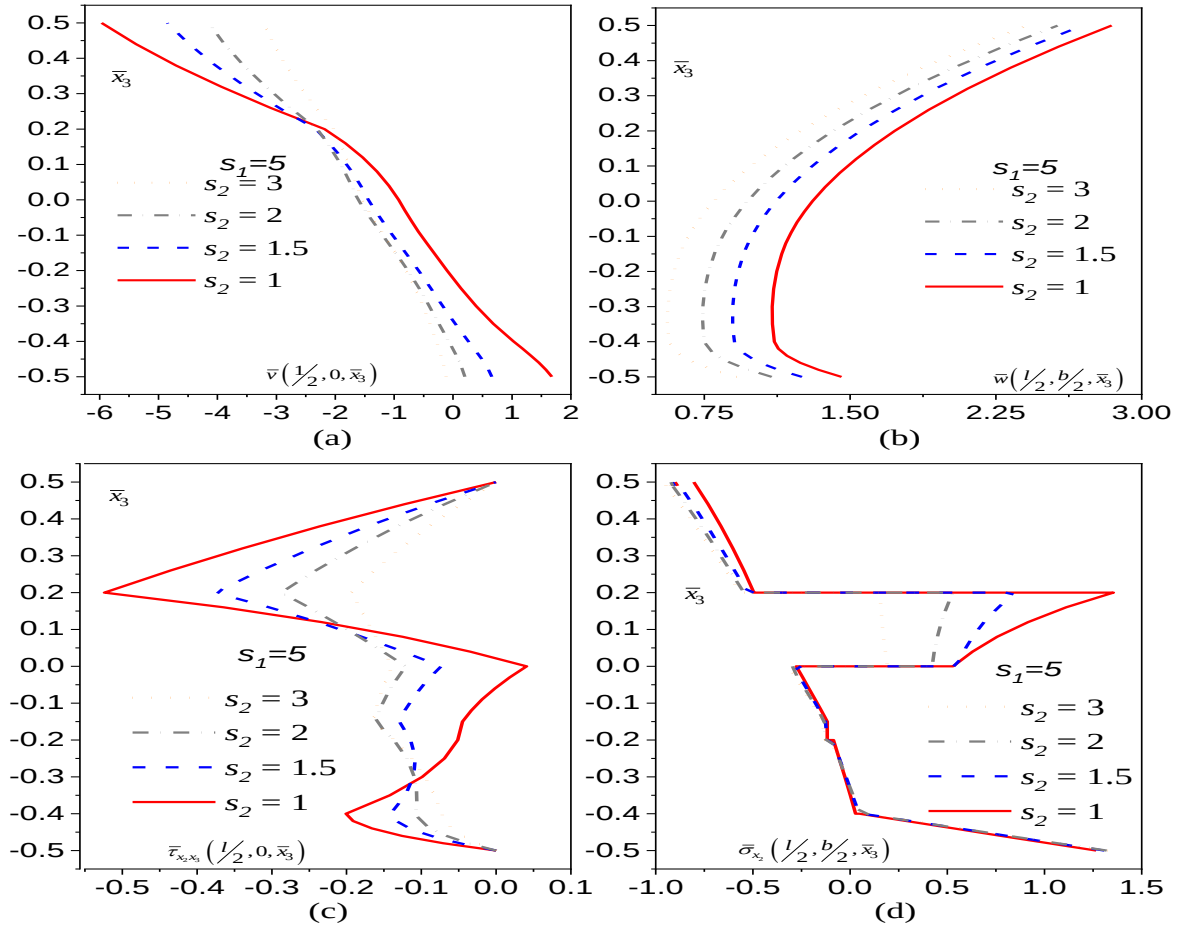

Fig. 10. Through thickness variation of normalized (a) in-plane displacement (b) transverse displacement (c) transverse shear stress (d) in-plane normal stress of five-layered homogeneous orthotropic laminate subjected to thermal load (Case II) for different in-plane (s_2) aspect ratio

The degree of orthotropic, lamination scheme, and transverse and in-plane aspect ratios are sensitive parameters toward the correct response prediction for laminated structures when subjected to thermal loading. The present formulation uses analytical and numerical approaches, achieving accuracy and simplicity.

It also helps to reduce the dimension of the elasticity problem and helps to avoid a complex 3D stress analysis. This unique formulation can analyze composite material subjected to environmental/externally imposed loads such as thermal, hygrothermal, piezoelectric, mechanical, and its combinations with little modification in the future.

Moreover, the application of present semi-analytical models for multi-directional FG materials can also be tested in the future. However, the presented formulation is restricted to simply supported boundary conditions and distributed transverse loading in bi-directional sinusoidal and uniform loading conditions.

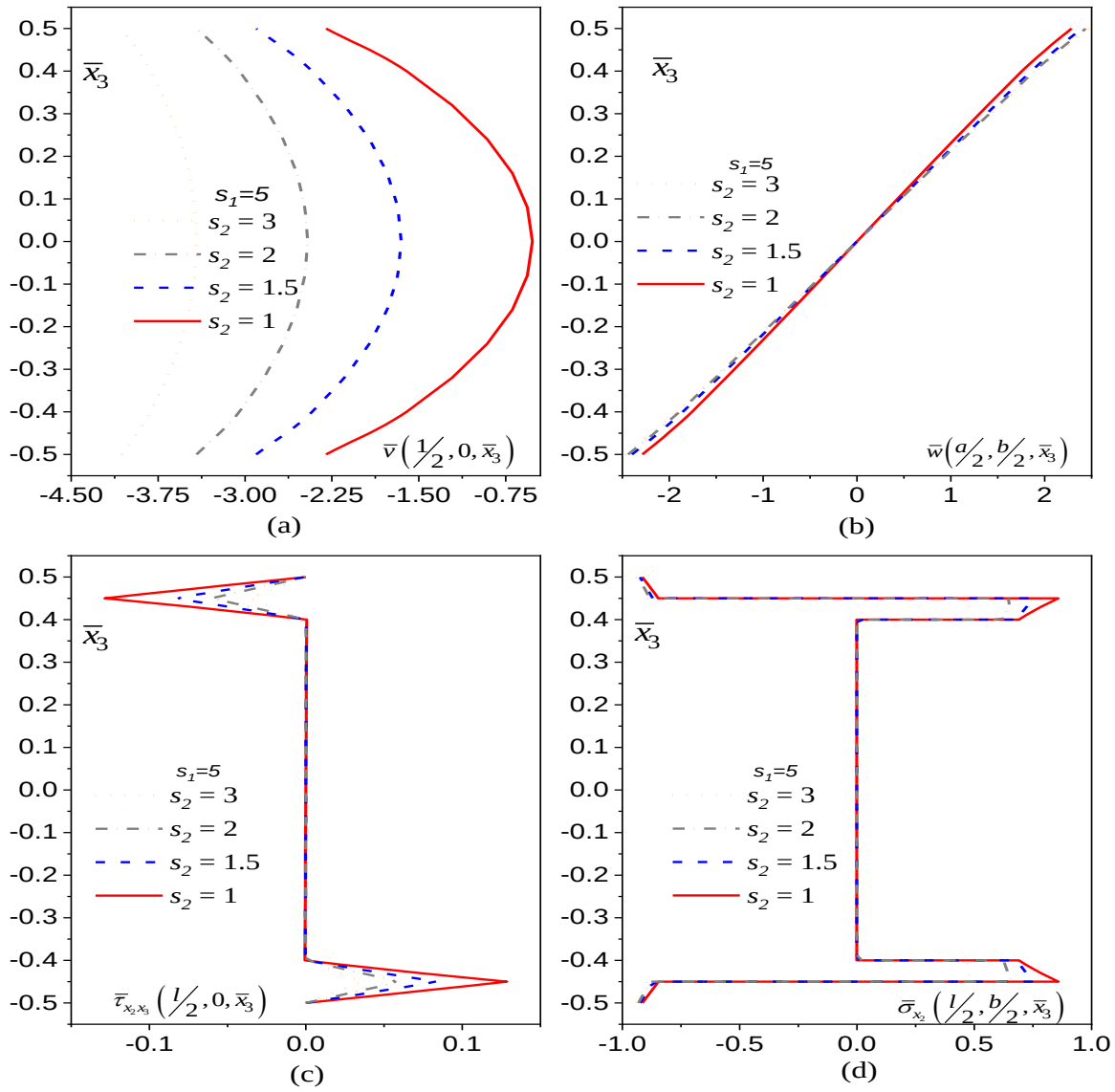

Fig. 11. Through thickness variation of normalized (a) in-plane displacement (b) transverse displacement (c) transverse shear stress (d) in-plane normal stress of five-layered sandwich composite laminate subjected to the thermal load, (Case I) for different in-plane aspect ratio

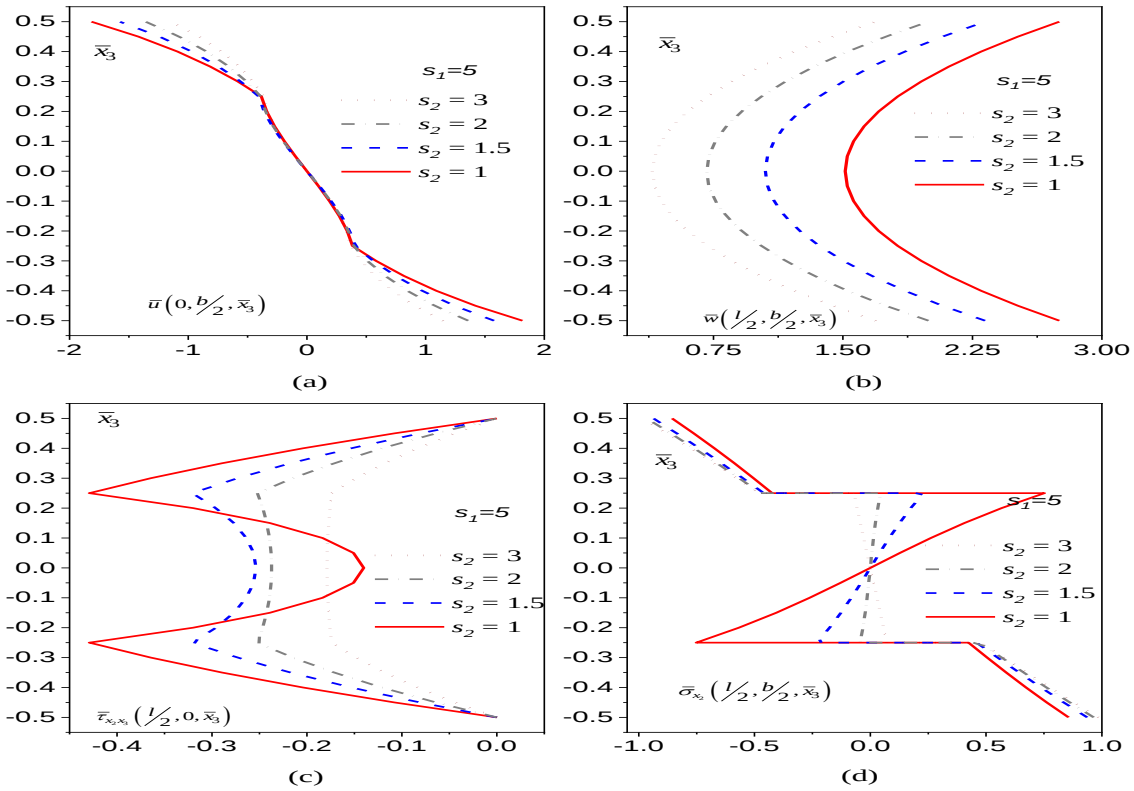

Fig. 12. Through thickness variation of normalized (a) in-plane displacement (b) transverse displacement (c) transverse shear stress (d) in-plane normal stress of four-layered symmetric laminate subjected to the thermal load, (Case II) for different in-plane aspect ratio

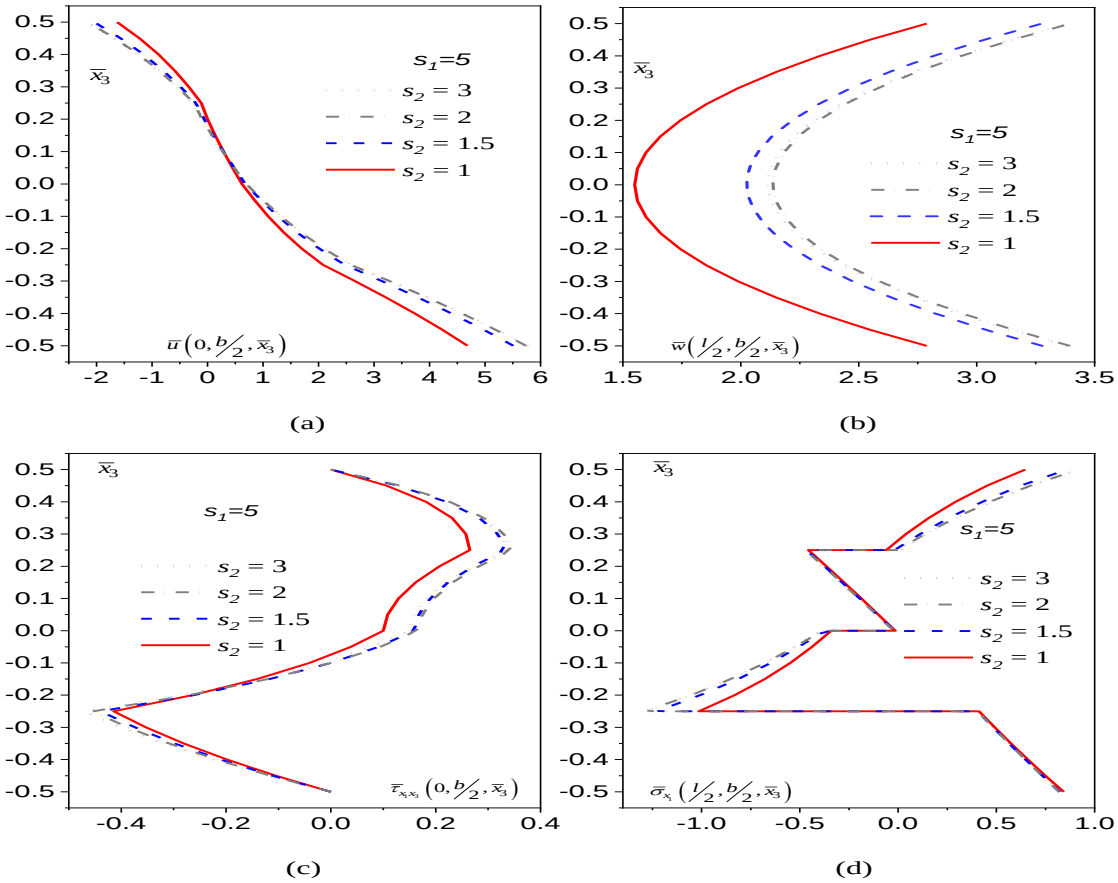

Fig. 13. Through thickness variation of normalized (a) in-plane displacement (b) transverse displacement (c) transverse shear stress (d) in-plane normal stress of four-layered anti-symmetric composite laminate subjected to the thermal load, (Case II) for different in-plane aspect ratio.

Table 5. In-plane normal stresses $(\bar{\sigma}_{X_1}, \bar{\sigma}_{X_2})$, transverse shear stresses $(\bar{\tau}_{X_1X_3}, \bar{\tau}_{X_2X_3})$, and the transverse displacement $(\bar{w})$ of five-layered $\left[0^0/0^0/0^0/90^0/0^0\right]$ orthotropic composite square laminates

	s	Source	$\bar{\sigma}_{X_1}\left(l/2, d/2\right)$	$\bar{\tau}_{X_1X_3}(0,0.2d)$	$\bar{w}\left(l/2, \mp d/2\right)$		$\bar{\sigma}_{X_2}\left(l/2, 0^+\right)$	$\bar{\tau}_{X_1X_2}\left(0, -0.4d^+\right)$	$\bar{\tau}_{X_2X_3}(0,0)$
Case I	5	[1]Exact solutions	0.6799	0.2610	-1.5802	2.3311	1.3365	-1.1570	0.3155
		Present Model 1	0.6803	0.2611	-1.5804	2.3319	1.3370	-1.1573	0.3156
		Present Model 2	0.8918	0.3281	-2.3291	2.6962	1.6647	-1.5978	0.4619
	10	[1]Exact solutions	0.3441	0.2083	-0.3989	0.7718	1.8825	-1.0761	0.5273
		Present Model 1	0.3442	0.2083	-0.3989	0.7719	1.8827	-1.0762	0.5274
		Present Model 2	0.3712	0.2159	-0.4805	0.7802	2.0083	-1.1836	0.5874
	20	[1]Exact solutions	0.1996	0.1595	0.0259	0.3351	2.0871	-1.0060	0.6292
		Present Model 1	0.1996	0.1595	0.0259	0.3351	2.0871	-1.0060	0.6292
		Present Model 2	0.2032	0.1597	0.0159	0.3312	2.1229	-1.0313	0.6471
	40	[1]Exact solutions	0.1564	0.1422	0.1461	0.2245	2.1452	-0.9812	0.6608
		Present Model 1	0.1564	0.1422	0.1461	0.2245	2.1452	-0.9812	0.6608
		Present Model 2	0.1571	0.1421	0.1444	0.2232	2.1545	-0.9874	0.6655
	s	Source	$\bar{\sigma}_{X_1}\left(l/2, d/2\right)$	$\bar{\tau}_{X_1X_3}(0,0.2\mathrm{d})$	$\bar{w}\left(l/2, 0\ \&\ d/2\right)$		$\bar{\sigma}_{X_2}\left(l/2, 0.2d^-\right)$	$\bar{\tau}_{X_1X_2}\left(0, -0.4d^+\right)$	$\bar{\tau}_{X_2X_3}(0,0.2d)$
Case II	5	[1]Exact solutions	0.8914	0.3787	1.3061	2.8454	1.3531	0.4574	-0.5237
		Present Model 1	0.8918	0.3788	1.3064	2.8461	1.3536	0.4574	-0.5239
		Present Model 2	0.8368	0.3702	1.5743	2.7791	0.9534	1.2766	-0.4846
	10	[1]Exact solutions	0.8037	0.5004	1.0784	1.4850	1.1968	0.2924	-0.6036
		Present Model 1	0.8038	0.5004	1.0784	1.4886	1.1969	0.2924	-0.6037
		Present Model 2	0.8877	0.5676	1.3723	1.6761	0.6143	0.9427	-0.5425
	20	[1]Exact solutions	0.7849	0.5501	0.9827	1.0872	1.1241	0.2237	-0.6291
		Present Model 1	0.7849	0.5501	0.9827	1.0872	1.1241	0.2236	-0.6291
		Present Model 2	0.9318	0.6595	1.2562	1.3324	0.4502	0.7967	-0.5629
	40	[1]Exact solutions	0.7810	0.5647	0.9547	0.9810	1.1020	0.2032	-0.6360
		Present Model 1	0.7810	0.5648	0.9547	0.9810	1.1020	0.2032	-0.6360
		Present Model 2	0.9469	0.6877	1.2195	1.2385	0.3993	0.7525	-0.5686

[1]Exact solutions = Kapuria and Achary [30]

Table 6. In-plane normal stresses $(\bar{\sigma}_{X_1}, \bar{\sigma}_{X_2})$, transverse shear stresses $(\bar{\tau}_{X_1X_3}, \bar{\tau}_{X_2X_3})$, and the transverse displacement $(\bar{w})$ of four-layered symmetric $\left[0^0/90^0/90^0/0^0\right]$ composite square laminates

	s	Source	$\bar{\sigma}_{X_1}\left(l/2, d/2\right)$	$\bar{\tau}_{X_1X_3}(0,-0.25\mathrm{d})$	$\bar{w}\left(l/2, \mp d/2\right)$		$\bar{\sigma}_{X_2}\left(l/2, -0.25d^+\right)$	$\bar{\tau}_{X_1X_2}\left(0, -d/2\right)$	$\bar{\tau}_{X_2X_3}(0,-0.25d)$
Case I	5	[1]Exact solutions	0.9134	-0.5603	-2.2777	2.2777	0.9186	-0.1426	0.5553
		Present Model 1	0.9138	-0.5605	-2.2784	2.2784	0.9190	-0.1427	0.5554
		Present Model 2	1.1023	-0.6678	-2.5672	2.5673	1.0011	-0.1598	0.5916
	10	[1]Exact solutions	0.8075	-0.6356	-0.6256	0.6256	0.8108	-0.0996	0.6338
		Present Model 1	0.8076	-0.6356	-0.6256	0.6256	0.8109	-0.0996	0.6338
		Present Model 2	0.8520	-0.6657	-0.6460	0.6460	0.8279	-0.1027	0.6452
	20	[1]Exact solutions	0.7753	-0.6572	-0.1604	0.1604	0.7763	-0.0868	0.6567
		Present Model 1	0.7753	-0.6572	-0.1604	0.1604	0.7763	-0.0868	0.6567
		Present Model 2	0.7862	-0.6649	-0.1617	0.1617	0.7803	-0.0875	0.6597
	40	[1]Exact solutions	0.7668	-0.6628	-0.0404	0.0404	0.7671	-0.0835	0.6627
		Present Model 1	0.7668	-0.6628	-0.0404	0.0404	0.7671	-0.0835	0.6627
		Present Model 2	0.7695	-0.6648	-0.0404	0.0404	0.7680	-0.0837	0.6634
	s	Source	$\bar{\sigma}_{X_1}\left(l/2, d/2\right)$	$\bar{\tau}_{X_1X_3}(0,0)$	$\bar{w}\left(l/2, -d/2\ \&\ 0\right)$		$\bar{\sigma}_{X_2}\left(l/2, -0.25d^+\right)$	$\bar{\tau}_{X_1X_2}\left(0, d/2\right)$	$\bar{\tau}_{X_2X_3}(0,0)$
Case II	5	[1]Exact solutions	0.7463	0.1933	2.7529	1.5126	-0.7510	-0.1316	-0.1403
		Present Model 1	0.7466	0.1933	2.7537	1.5131	-0.7513	-0.1317	-0.1403
		Present Model 2	0.7745	0.1934	2.8210	1.5399	-0.7646	-0.1348	-0.1463
	10	[1]Exact solutions	0.7524	0.2850	1.6449	1.3250	-0.5152	-0.0975	-0.2632
		Present Model 1	0.7525	0.2850	1.6450	1.3251	-0.5152	-0.0975	-0.2632
		Present Model 2	0.7593	0.2855	1.6554	1.3329	-0.5175	-0.0981	-0.2652
	20	[1]Exact solutions	0.7603	0.3193	1.3155	1.2349	-0.4192	-0.0864	-0.3130
		Present Model 1	0.7603	0.3193	1.3155	1.2349	-0.4192	-0.0864	-0.3130
		Present Model 2	0.7621	0.3195	1.3177	1.2368	-0.4196	-0.0865	-0.3136
	40	[1]Exact solutions	0.7630	0.3290	1.2283	1.2081	-0.3916	-0.0834	-0.3274
		Present Model 1	0.7630	0.3290	1.2284	1.2081	-0.3915	-0.0834	-0.3274
		Present Model 2	0.7634	0.3291	1.2289	1.2086	-0.3917	-0.0834	-0.3275

[1]Exact solutions = Kapuria and Achary [30]

Table 7. In-plane normal stresses ($\bar{\sigma}_{x_1}, \bar{\sigma}_{x_2}$), transverse shear stresses ($\bar{\tau}_{x_1x_3}, \bar{\tau}_{x_2x_3}$), and the transverse displacement ($\bar{w}$) of four-layered anti-symmetric $\left[90^0/0^0/90^0/0^0\right]$ composite square laminates

	s	Source	$\bar{\sigma}_{x_1}\left(l/2, d/2\right)$	$\bar{\tau}_{x_1x_3}(0, 0.25d)$	$\bar{w}\left(l/2, \mp d/2\right)$		$\bar{\sigma}_{x_2}\left(l/2, -d/2\right)$	$\bar{\tau}_{x_1x_2}\left(0, -d/2\right)$	$\bar{\tau}_{x_2x_3}(0, -0.25d)$
Case I		[1]Exact solutions	0.8549	0.5091	-2.2801	2.2801	0.8549	-0.1429	-0.5091
	5	Present Model 1	0.8553	0.5093	-2.2808	2.2808	0.8553	-0.1429	-0.5093
		Present Model 2	1.0176	0.5936	-2.5707	2.5707	1.0176	-0.1601	-0.5936
		[1]Exact solutions	0.7771	0.6110	-0.6257	0.6257	0.7771	-0.0996	-0.6110
	10	Present Model 1	0.7771	0.6111	-0.6257	0.6257	0.7772	-0.0996	-0.6111
		Present Model 2	0.8137	0.6347	-0.6461	0.6461	0.8137	-0.1028	-0.6347
		[1]Exact solutions	0.7657	0.6496	-0.1604	0.1604	0.7657	-0.0868	-0.6497
	20	Present Model 1	0.7657	0.6496	-0.1604	0.1604	0.7657	-0.0868	-0.6496
		Present Model 2	0.7745	0.6557	-0.1617	0.1617	0.7745	-0.0875	-0.6557
		[1]Exact solutions	0.7643	0.6608	-0.0404	0.0404	0.7643	-0.0835	-0.6608
	40	Present Model 1	0.7643	0.6608	-0.0404	0.0404	0.7643	-0.0835	-0.6608
		Present Model 2	0.7664	0.6623	-0.0404	0.0404	0.7664	-0.0837	-0.6623
	s	Source	$\bar{\sigma}_{x_1}\left(l/2, d/2\right)$	$\bar{\tau}_{x_1x_3}(0, 0.25d)$	$\bar{w}\left(l/2, -d/2\ \&\ 0\right)$		$\bar{\sigma}_{y}\left(l/2, d/2\right)$	$\bar{\tau}_{x_1x_2}\left(0, d/2\right)$	$\bar{\tau}_{x_2x_3}(0, 0.25d)$
Case II		[1]Exact solutions	0.6473	0.2648	2.7869	1.5492	-0.8426	-0.1380	-0.4145
	5	Present Model 1	0.6476	0.2649	2.7878	1.5497	-0.8426	-0.1380	-0.4146
		Present Model 2	0.6737	0.2735	2.8557	1.5772	-0.8389	-0.1413	-0.4248
		[1]Exact solutions	0.5917	0.2942	1.8455	1.5276	-0.8768	-0.1130	-0.4471
	10	Present Model 1	0.5918	0.2942	1.8457	1.5277	-0.8768	-0.1130	-0.4471
		Present Model 2	0.5979	0.2966	1.8569	1.5364	-0.8760	-0.1137	-0.4499
		[1]Exact solutions	0.5759	0.3025	1.5937	1.5136	-0.8863	-0.1060	-0.4561
	20	Present Model 1	0.5759	0.3025	1.5937	1.5137	-0.8863	-0.1060	-0.4561
		Present Model 2	0.5774	0.3031	1.5961	1.5159	-0.8861	-0.1062	-0.4568
		[1]Exact solutions	0.5718	0.3046	1.5296	1.5095	-0.8888	-0.1042	-0.4584
	40	Present Model 1	0.5718	0.3046	1.5296	1.5095	-0.8888	-0.1042	-0.4584
		Present Model 2	0.5722	0.3047	1.5302	1.5101	-0.8887	-0.1043	-0.4586

[1]Exact solutions = Kapuria and Achary [30]

Table 8. In-plane normal stresses ($\bar{\sigma}_{x_1}, \bar{\sigma}_{x_2}$), transverse shear stresses ($\bar{\tau}_{x_1x_3}, \bar{\tau}_{x_2x_3}$), and the transverse displacement ($\bar{w}$) of five-layered sandwich composite square laminates

	s	Source	$\bar{\sigma}_{x_1}\left(l/2, -d/2\right)$	$\bar{\tau}_{x_1x_3}(0, -0.45d)$	$\bar{w}\left(l/2, \mp d/2\right)$		$\bar{\sigma}_{x_2}\left(l/2, -0.45d^+\right)$	$\bar{\tau}_{x_1x_2}\left(0, -d/2\right)$	$\bar{\tau}_{x_2x_3}(0, -0.45d)$
Case I		[1]Exact solutions	0.7973	-0.1215	-2.2860	2.2860	0.8580	-0.0679	0.1285
	5	Present Model 1	0.7974	-0.1215	-2.2867	2.2867	0.8580	-0.0679	0.1285
		Present Model 2	2.5120	-0.3997	-2.7229	2.7271	2.1455	-0.7503	0.1070
		[1]Exact solutions	0.8045	-0.1322	-0.6544	0.6544	0.8220	-0.0633	0.1338
	10	Present Model 1	0.8045	-0.1321	-0.6545	0.6545	0.8220	-0.0633	0.1338
		Present Model 2	2.0543	-0.3372	-0.6792	0.6871	1.7637	-0.1222	0.1155
		[1]Exact solutions	0.8068	-0.1354	-0.1699	0.1699	0.8112	-0.0620	0.1354
	20	Present Model 1	0.8068	-0.1354	-0.1699	0.1699	0.8112	-0.0620	0.1354
		Present Model 2	1.9337	-0.3207	-0.1665	0.1753	1.6676	-0.1151	0.1171
		[1]Exact solutions	0.8075	-0.1362	-0.0429	0.0429	0.8084	-0.0616	0.1359
	40	Present Model 1	0.8075	-0.1362	-0.0429	0.0429	0.8084	-0.0616	0.1359
		Present Model 2	1.9032	-0.3165	-0.0382	0.0472	1.6435	-0.1133	0.1182
	s	Source	$\bar{\sigma}_{x_1}\left(l/2, 0.45d\right)$	$\bar{\tau}_{x_1x_3}(0, -0.45d)$	$\bar{w}\left(l/2, -d/2\ \&\ 0\right)$		$\bar{\sigma}_{x_2}\left(l/2, d/2\right)$	$\bar{\tau}_{x_1x_2}\left(0, -d/2\right)$	$\bar{\tau}_{x_2x_3}(0, -0.45d)$
Case II		[1]Exact solutions	-0.6455	0.0817	1.6070	0.7887	-0.9357	0.0513	-0.1161
	5	Present Model 1	-0.6455	0.0817	1.6071	0.7887	-0.9357	0.0513	-0.1161
		Present Model 2	1.3497	0.1978	2.8026	1.4228	1.2760	0.4752	-0.1177
		[1]Exact solutions	-0.6486	0.0890	1.1075	0.8991	-0.9411	0.0491	-0.1173
	10	Present Model 1	-0.6485	0.0890	1.1075	0.8991	-0.9411	0.0491	-0.1173
		Present Model 2	1.2902	0.1919	1.9804	1.6352	1.2116	0.8947	-0.1192
		[1]Exact solutions	-0.6487	0.0938	0.9821	0.9298	-0.9432	0.0485	-0.1177
	20	Present Model 1	-0.6487	0.0938	0.9821	0.9298	-0.9432	0.0485	-0.1177
		Present Model 2	1.2752	0.1904	1.7749	1.6886	1.1953	1.7611	-0.1196
		[1]Exact solutions	-0.6486	0.0956	0.9510	0.9379	-0.9439	0.0483	-0.1178
	40	Present Model 1	-0.6486	0.0956	0.9510	0.9379	-0.9439	0.0483	-0.1178
		Present Model 2	1.2714	0.1900	1.7235	1.7020	1.1912	3.5082	-0.1197

[1]Exact solutions = Kapuria and Achary [30]

Table 9. In-plane normal stresses, transverse shear stresses ($\bar{\tau}_{x_1x_3}, \bar{\tau}_{x_2x_3}$), and the transverse displacement ($\bar{w}$) of four-layered symmetric $\left[0^0/90^0/90^0/0^0\right]$ composite rectangular ($b/l = 2$) laminates

	s	Source	$\bar{\sigma}_{x_1}\left(l/2, -d/2\right)$	$\bar{\tau}_{x_1x_3}\left(0, -d/4\right)$	$\bar{w}\left(l/2, \mp d/2\right)$		$\bar{\sigma}_{x_2}\left(l/2, 0\right)$	$\bar{\tau}_{x_1x_2}\left(0, -d/2\right)$	$\bar{\tau}_{x_2x_3}\left(0, -0.25d\right)$
Case I		[1]Exact solutions	1.0756	-0.6300	-2.3984	2.3984	0.4826	-0.1197	0.2685
	5	Present Model 1	1.0758	-0.6301	-2.3989	2.3989	0.4828	-0.1197	0.2686
		Present Model 2	1.1930	-0.6942	-2.5710	2.5710	0.4948	-0.1273	0.2794
		[1]Exact solutions	0.9038	-0.6764	-0.6354	0.6354	0.5529	-0.0979	0.2900
	10	Present Model 1	0.9039	-0.6764	-0.6355	0.6355	0.5530	-0.0979	0.2900
		Present Model 2	0.9301	-0.6935	-0.6470	0.6470	0.5572	-0.0995	0.2931
		[1]Exact solutions	0.8546	-0.6888	-0.1613	0.1613	0.5723	-0.0919	0.2959
	20	Present Model 1	0.8546	-0.6888	-0.1613	0.1613	0.5723	-0.0919	0.2959
		Present Model 2	0.8609	-0.6931	-0.1620	0.1620	0.5735	-0.0922	0.2966
		[1]Exact solutions	0.8418	-0.6920	-0.0405	0.0405	0.5773	-0.0903	0.2974
	40	Present Model 1	0.8418	-0.6920	-0.0405	0.0405	0.5773	-0.0903	0.2974
		Present Model 2	0.8434	-0.6931	-0.0405	0.0405	0.5776	-0.0904	0.2976
	s	Source	$\bar{\sigma}_{x_1}\left(l/2, -d/2\right)$	$\bar{\tau}_{x_1x_3}\left(0,0\right)$	$\bar{w}\left(l/2, -d/2\ \&\ 0\right)$		$\bar{\sigma}_{x_2}\left(l/2, -d/2\right)$	$\bar{\tau}_{x_1x_2}\left(0, -d/2\right)$	$\bar{\tau}_{x_2x_3}\left(0,0\right)$
Case II		[1]Exact solutions	-0.4641	0.0101	1.9951	0.7105	0.9653	0.0529	-0.2371
	5	Present Model 1	-0.4643	0.0101	1.9956	0.7107	0.9652	0.0530	-0.2371
		Present Model 2	-0.4796	0.0077	2.0316	0.7176	0.9645	0.0539	-0.2419
		[1]Exact solutions	-0.3879	0.0259	1.0780	0.7504	0.9796	0.0332	-0.2693
	10	Present Model 1	-0.3879	0.0259	1.0781	0.7504	0.9796	0.0332	-0.2693
		Present Model 2	-0.3914	0.0253	1.0833	0.7538	0.9795	0.0334	-0.2707
		[1]Exact solutions	-0.3664	0.0305	0.8333	0.7509	0.9836	0.0277	-0.2787
	20	Present Model 1	-0.3664	0.0305	0.8333	0.7509	0.9836	0.0277	-0.2787
		Present Model 2	-0.3673	0.0304	0.8343	0.7519	0.9836	0.0277	-0.2790
		[1]Exact solutions	-0.3609	0.0318	0.7710	0.7504	0.9847	0.0263	-0.2812
	40	Present Model 1	-0.3609	0.0317	0.7710	0.7504	0.9847	0.0262	-0.2811
		Present Model 2	-0.3611	0.0317	0.7712	0.7506	0.9847	0.0263	-0.2812

[1]Exact solutions = Kapuria and Achary [30]

Conflicts of Interest

The author declares that there is no conflict of interest regarding the publication of this manuscript. In addition, the authors have entirely observed the ethical issues, including plagiarism, informed consent, misconduct, data fabrication and/or falsification, double publication and/or submission, and redundancy.

References

[1] Pell, W.H., 1946. Thermal deflection of anisotropic thin plates. *Quarterly of Applied Mathematics,*4, pp. 27-44.

[2] Timoshenko, S. and Woinowsky-Krieger, S., 1959.Theory of plates and shells, 2nd Edition, *McGraw-Hill*, New York.

[3] Boley, B.A. and Weiner, J.H., 1960. Theory of thermal stresses. *Wiley*, New York.

[4] Johns, D.J., 1965. Thermal stress analyses. *Pergamon*, Oxford.

[5] Parkus H, 1968. Thermoelasticity, Blaisdell, Waltham, MA.

[6] Burgreen, D., 1971. Elements of thermal stress analysis. *NYCP Press*, Jamaica.

[7] Vinson, J.R., 1974. Structural Mechanics: The behaviour of plates and shells. *Wiley*, New York.

[8] Srinivas, S. and Rao, A.K,, 1972. A note of flexure of thick rectangular plates and laminates with the variation of temperature across thickness. *Bulletin of the Polish Academy of Sciences – Technical Sciences* (20), pp. 229 – 234.

[9] Boley, B.A., 1972. On thermal stresses in beams: Some limitations of the elementary theory. *International Journal of solid structures*, (8), pp. 571-579.

[10] Bapu Rao, M.N., 1979(a). Thermal Bending of Thick Rectangular Plates Nuclear Engineering and Design (54), pp.115-118.

[11] Bapu Rao, M.N., 1979(b). Three-Dimensional analysis of thermally loaded thick plates Nuclear Engineering and Design (55), pp. 353-361.

[12] Tungikar, V.B. and Rao, K.M., 1994. Three-Dimensional exact solution of thermal stresses in rectangular composite laminate. *Composite Structures* (27), pp. 419-430.

[13] Wu, C.H. and Tauchert, T.R., 1980. Thermoelastic analysis of laminated plates: 1, Symmetric specially orthotropic laminates. *Journal of Thermal Stresses* (3), pp. 247-249.

[14] Reddy JN and Chao WC, 1980. Finite element analysis of laminated bi-modulus composite material plates, *Computers and Structures*, (12), pp. 245 -257.

[15] Reddy, J.N., Bert, C.W., Hsu, Y.S. and Reddy, V.S., 1980. Thermal bending of thick rectangular plates of bi-modules composite materials. *Journal of Mechanical Engineering Science*, (22), pp. 297-304.

[16] Carrera, E., 2000. An assessment of mixed and classical theories for the thermal stress analysis of orthotropic multilayered plates. *Journal of thermal stresses*, *23*(9), pp.797-831.

[17] Allam, O., Draiche, K., Bousahla, A.A., Bourada, F., Tounsi, A., Benrahou, K.H., Mahmoud, S.R., Bedia, E.A. and Tounsi, A., 2020. A generalized 4-unknown refined theory for bending and free vibration analysis of laminated composite and sandwich plates and shells. *Computers and Concrete, An International Journal*, *26*(2), pp.185-201.

[18] Kouider, D., Kaci, A., Selim, M.M., Bousahla, A.A., Bourada, F., Tounsi, A., Tounsi, A. and Hussain, M., 2021. An original four-variable quasi-3D shear deformation theory for the static and free vibration analysis of new type of sandwich plates with both FG face sheets and FGM hard core. *Steel and Composite Structures*, *41*(2), pp.167-191.

[19] Burton. and Noor, A.K., 1992. Computational models for high-temperature multilayered composite plates and shells. *Applied Mechanics*, 45(10) - 419.

[20] Jonalagadda, K.D., Tauchert, T.R. and Blandford, G.E., 1993. Higher-order thermoelastic composite plate theories: An analytical comparison. *Journal of Thermal stresses*, (16), pp. 265-284.

[21] Savoia, M. and Reddy, J.N., 1995. Three-dimensional thermal analysis of laminated composite plates. *International Journal of Solids and Structures*, 32(5), pp. 593-608.

[22] Bhaskar, K., Varadan, T.K. and Ali, J.S.M., 1996. thermoelastic solutions for orthotropic and anisotropic composite laminates. *Composites: Part B*, (27), pp. 415-420.

[23] Rolfes, R., Noor, A.K. and Sparr, H., 1998. Evaluation of transverse thermal stresses in composite plates based on first-order shear deformation theory. *Computer Methods in Applied Mechanics and Engineering*, (167), pp. 355-368.

[24] Abualnour, M., Chikh, A., Hebali, H., Kaci, A., Tounsi, A., Bousahla, A. A., and Tounsi, A. 2019. Thermomechanical analysis of antisymmetric laminated reinforced composite plates using a new four variable trigonometric refined plate theory. Computers and Concrete, 24(6), 489–498.

[25] Bakoura, A., Djedid, I.K., Bourada, F., Bousahla, A.A., Mahmoud, S.R., Tounsi, A., Ghazwani, M.H. and Alnujaie, A., 2022. A mechanical behavior of composite plates using a simple three variable refined plate theory. *Structural engineering and mechanics*, *83*(5), pp.617-625.

[26] Carrera,, E., 2002. Temperature profile influence on layered plates response considering classical and advanced theories. *AIAA journal*, *40*(9), pp.1885-1896.

[27] Carrera, E. and Ciuffreda, A., 2004. Closed-form solutions to assess multilayered-plate theories for various thermal stress problems. *Journal of Thermal Stresses*, *27*(11), pp.1001-1031.

[28] Robaldo, A. and Carrera, E., 2007. Mixed finite elements for thermoelastic analysis of multilayered anisotropic plates. *Journal of Thermal Stresses*, *30*(2), pp.165-194.

[29] Kapuria, S., Dumir, P.C., and Ahmed, A,, 2003. An efficient higher-order zigzag theory for composite and sandwich beams subjected to thermal loading. *International Journal of Solids and Structures*. (40), pp. 6613-6631

[30] Kapuria, S. and Achary, G.G.S. 2004. An efficient higher-order zigzag theory for laminated plates subjected to thermal loading. *International Journal of Solids and Structures*, (41), pp. 4661-4684.

[31] Robaldo, A, Carrera, E., and Benjeddou, A., Thermoelastic analysis of multilayered anisotropic composite plates. *Journal of Thermal Stresses*, (28), pp. 1031-1065.

[32] Pradeep, V., Ganesan, N. and Bhaskar, K., 2006. Vibration and thermal buckling of composite sandwich beams with viscoelastic core. *Composite Structures* 2007, 81: 60–69.

[33] Gherlone, M. and Sciuva, M., 2007. Thermo-mechanics of undamaged and damaged multilayered composite plates: a sub-laminates finite element approach. *Composite Structures*, (81), pp. 125–136.

[34] Kant, T., Pendhari, S.S. and Desai, Y.M., 2007. Two-Dimensional stress analyses of laminates under thermal load. *Proceedings of Indian National Science Academy*, 73(3), pp. 137-145.

[35] Kant, T., Pendhari, S.S. and Desai, Y.M., 2008. An efficient semi-analytical model for composite and sandwich plates subjected to thermal load, *Journal of Thermal Stresses*, (31), pp. 77–103.

[36] Pradeep, V. and Ganesan, N., 2008. Thermal buckling and vibration behaviour of multi-layer rectangular viscoelastic sandwich plates. *Journal of Sound and Vibration*, (310), pp. 169–183.

[37] Pagani, A. and Carrera, E., 2017. Large-deflection and post-buckling analyses of laminated composite beams by Carrera Unified Formulation, *Composite Structures*, (170),Pages 40-52.

[38] Sur, A. and Kanoria, M., 2018. Thermoelastic interaction in a three-dimensional layered sandwich structure. *Mechanics of Advanced Composite Structures*, 5(2), 187-198.

[39] Garg, A. and Chalak, H. D., 2019. A review on analysis of laminated composite and sandwich structures under hygrothermal conditions. *Thin-Walled Structures,* 142, 205-226.

[40] Garg, A. and Chalak, H., 2021. Analysis of non-skew and skew laminated composite and sandwich plates under hygro-thermo-mechanical conditions including transverse stress variations. *Journal of Sandwich Structures & Materials*, 23(8), pp. 3471–3494

[41] Naik, N. and Sayyad, A., 2021. Higher-order displacement model for cylindrical bending of laminated and sandwich plates subjected to environmental loads. *Mechanics of Advanced Composite Structures*, 8(1), pp. 185-201.

[42] Kant, T. and Shiyekar, S.M., 2013. An assessment of a higher-order theory for composite laminates subjected to thermal gradient. *Composite Structures*, (96), pp. 698–707.

[43] Ghugal, Y.M. and Kulkarni, S.K., 2013. Thermal flexural analysis of cross-ply laminated plates using trigonometric shear deformation theory. *Latin American Journal of Solids and Structures*, (10), pp. 1001 – 1023.

[44] Ghugal, Y.M. and Kulkarni, S.K., 2013. Thermal response of symmetric cross-ply laminated plates subjected to linear and non-linear thermo-mechanical loads. *Journal of Thermal Stresses,* (36), pp. 466 – 479.

[45] Sayyad, A.S., Shinde, B.M. and Ghugal, Y.M., 2013. Thermoelastic bending analysis of orthotropic plates using hyperbolic shear deformation theory. *Composites: Mechanics, Computations, Applications. An International Journal*, 4(3), pp. 257 – 278.

[46] Norouzi, M., Delouei, A.A. and Seilsepour, M., 2013. A general exact solution for heat conduction in multilayer spherical composite laminates. *Composite Structures*, (106), pp. 288 – 295.

[47] Parviz, M., Vosoughi, A.R., Sadeghpour, M. and Hamid, R. V., 2014. Thermal buckling optimization of temperature-dependent laminated composite skew plates. *Journal of Aerospace Engineering* (27), pp. 64-75.

[48] Sayyad, A.S., Ghugal. Y.M. and Shinde, B.M., 2016. Thermal stress analysis of laminated composite plates using exponential shear deformation theory. *International Journal of Automotive Composites*. (2), pp. 23 – 40.

[49] Sayyad, A.S., Ghugal, Y.M. and Mhaske, B.A., 2015. A four-variable plate theory for thermoelastic bending analysis of laminated composite plates. *Journal of Thermal Stresses*. (38), pp. 904 – 925.

[50] Jafari, M. and Jafari, M., 2018. Effect of hole geometry on the thermal stress analysis of perforated composite plate under uniform heat flux. *Journal of Composite Materials*, pp. 1 – 17.

[51] Fazzolari, F.A. and Carrera, E., 2014. Thermal stability of FGM sandwich plates under various through-the-thickness temperature distributions. *Journal of Thermal Stresses*, *37*(12), pp.1449-1481.

[52] Tahir, S.I., Tounsi, A., Chikh, A., Al-Osta, M.A., Al-Dulaijan, S.U. and Al-Zahrani, M.M., 2022. The effect of three-variable viscoelastic foundation on the wave propagation in functionally graded sandwich plates via a simple quasi-3D HSDT. *Steel and Composite Structures*, *42*(4), p.501.

[53] Zaitoun, M.W., Chikh, A., Tounsi, A., Al-Osta, M.A., Sharif, A., Al-Dulaijan, S.U. and Al-Zahrani, M.M., 2022. Influence of the visco-Pasternak foundation parameters on the

buckling behavior of a sandwich functional graded ceramic–metal plate in a hygrothermal environment. *Thin-Walled Structures*, *170*, p.108549.

[54] Bendenia, N., Zidour, M., Bousahla, A.A., Bourada, F., Tounsi, A., Benrahou, K.H., Bedia, E.A., Mahmoud, S.R. and Tounsi, A., 2020. Deflections, stresses and free vibration studies of FG-CNT reinforced sandwich plates resting on Pasternak elastic foundation. *Computers and Concrete, An International Journal*, *26*(3), pp.213-226

[55] Kant, T. and Ramesh, C.K., 1981. Numerical integration of linear boundary value problems in solid mechanics by segmentation method. International Journal for Numerical Methods in Engineering, 17(8), pp.1233-1256.